PB85-181840

SO2 Concentration Estimates for New York City, 1880-1980

Washington Univ., St. Louis, MO

Prepared for

Environmental Protection Agency
Research Triangle Park, NC

Apr 85

U.S. Department of Commerce
National Technical Information Service
NTIS

PB85-181840

EPA/600/3-85/024
April 1985

SO_2 CONCENTRATION ESTIMATES FOR NEW YORK CITY, 1880-1980

by

R.B. Husar and D.E. Patterson
Center for Air Pollution Impact
and Trend Analysis
Washington University
St. Louis, MO 63130

68-02-3746

Project Officer

John W. Spence
Emissions Measurements and Characterization Division
Atmospheric Sciences Research Laboratory
Research Triangle Park, NC 27711

ATMOSPHERIC SCIENCES RESEARCH LABORATORY
OFFICE OF RESEARCH AND DEVELOPMENT
U.S. ENVIRONMENTAL PROTECTION AGENCY
RESEARCH TRIANGLE PARK, NC 27711

REPRODUCED BY
NATIONAL TECHNICAL
INFORMATION SERVICE
U.S. DEPARTMENT OF COMMERCE
SPRINGFIELD, VA. 22161

TECHNICAL REPORT DATA
(Please read Instructions on the reverse before completing)

1. REPORT NO. EPA/600/3-85/024	2.
3. RECIPIENT'S ACCESSION NO. PB85 181840 AS	
4. TITLE AND SUBTITLE SO_2 CONCENTRATION ESTIMATES FOR NEW YORK CITY, 1880-1980	5. REPORT DATE April 1985
	6. PERFORMING ORGANIZATION CODE
7. AUTHOR(S) R. Husar and D. Patterson	8. PERFORMING ORGANIZATION REPORT NO.
9. PERFORMING ORGANIZATION NAME AND ADDRESS Center for Air Pollution Impact and Trend Analysis Washington University St. Louis, MO 63130	10. PROGRAM ELEMENT NO. CCVN1A-09/2107 (FY-85)
	11. CONTRACT/GRANT NO. 68-02-3746
12. SPONSORING AGENCY NAME AND ADDRESS Atmospheric Sciences Research Laboratory - RTP, NC Office of Research and Development U.S. Environmental Protection Agency Research Triangle Park, N.C. 27711	13. TYPE OF REPORT AND PERIOD COVERED Final
	14. SPONSORING AGENCY CODE EPA/600/09
15. SUPPLEMENTARY NOTES	

16. ABSTRACT

The purpose of this investigation was to estimate the yearly ambient concentration of SO_2 and SO_4 wet deposition from 1880 to 1980 for the greater New York City area. This information was used to reconstruct ambient concentrations at two New York Veterans Administration cemeteries, Cypress Hills and Long Island, for studying marble deterioration. This study which involved a determination of marble loss rate as a function of SO_2 concentrations is the subject of another report. The methodology for developing the retrospective model to estimate yearly ambient concentrations since the turn of the century for the greater New York City area is presented in this report. The retrospective estimation of sulfur concentration and deposition required estimation of both local and regional emission trends since the turn of the century, along with suitable choice of a local and a regional dispersion model to relate emissions to ambient concentrations and deposition. The retrospective estimates are compared to observed SO_2 concentrations. It needs no elaboration that the estimation of local and regional emissions pertinent to a given receptor, the quantification of the local and regional contributions to SO_2 and to the wet deposition, and reconciliation with existing observations is a formidable task. Lacking data for the historical trends, many of the assumptions are based on "best available science", and they should be revised with the availability of new knowledge.

17. KEY WORDS AND DOCUMENT ANALYSIS

a. DESCRIPTORS	b. IDENTIFIERS/OPEN ENDED TERMS	c. COSATI Field/Group

18. DISTRIBUTION STATEMENT RELEASE TO PUBLIC	19. SECURITY CLASS *(This Report)* UNCLASSIFIED	21. NO. OF PAGES 36
	20. SECURITY CLASS *(This page)* UNCLASSIFIED	22. PRICE

EPA Form 2220-1 (Rev. 4-77) PREVIOUS EDITION IS OBSOLETE

NOTICE

The information in this document has been funded by the United States Environmental Protection Agency under Contract 68-02-3746 to Washington University. It has been subject to the Agency's peer and administrative review, and it has been approved for publication as an EPA document. Mention of trade names or commercial products does not constitute endorsement or recommendation for use.

ABSTRACT

The purpose of this investigation is to estimate the ambient concentration effects of SO_2 for two sites in the greater New York City area, one with high and another with lower SO_2 concentration history, and to compare the marble loss rate at the two sites Cypress Hills and Long Island. Choosing geographically close locations effectively eliminates the natural weathering as a significant variable, as well as regional scale air pollution influence. Hence, in this case the differences in the weathering rates are reasonably attributable to the man-induced local air pollution. The marble loss rates and the estimated SO_2 concentration histories at the two sites permit a crude estimate of the damage function, i.e. loss rate increase per SO_2 concentration increase.

The current investigation of tombstone weathering rates is broken down into two parts: (1) Retrospective reconstruction of the chemical environment (SO_2 concentration and SO_4 wet deposition); (2) Marble loss rate as a function of SO_2 concentration. The present report is devoted to part 1.

The retrospective estimation of sulfur concentration and deposition requires estimation of both local and regional emission trends since the turn of the century, along with suitable choice of a local and a regional dispersion model to relate emissions to ambient concentration and deposition. The retrospective estimates are compared to observed SO_2 concentrations.

It needs no elaboration that the estimation of local and regional emissions pertinent to a given receptor, the quantification of the local and regional contributions to SO_2 and to the wet deposition, and reconciliation of the above with the existing observations is a formidable task for current conditions. This, however, does not diminish the need for such estimates. Lacking data for the historical trends, many of the assumptions here are based on intuition or "best available science", and they should be revised with the availability of new knowledge.

TABLE OF CONTENTS

Abstract iii
List of Figures vi
Acknowledgements viii
1. Introduction 1
2. Methodology for Retrospective Air Pollution Analysis 1
3. Ambient Concentrations of Sulfur Compounds 4
SO_2 concentration measurements 4
Haziness 5
4. Sulfur Emission Trends Affecting the New York Area 8
New York area trends 8
Eastern North American trends 12
5. Regional Model 16
Transport 17
Kinetics 19
Application 19
6. Reconciliation of Data and Model Estimates 23
7. Discussion 29
REFERENCES 29

LIST OF FIGURES

1. Schematic illustration of the mass balance approach to pollutant flow 3

2. Fifteen year trend of sulfur dioxide concentration in Central Park, adopted from Eisenbud et. al. (1973) 5

3. Observed SO_2 concentration fields for the New York City area from Eisenbud, et. al.,(a) January, 1969; (b) July, 1970 6

4. Diurnal SO_2 concentration for New York City, 1957-1967 7

5. Seasonal SO_2 concentration for New York City, 1957-1967 7

6. Trend of winter quarter haziness at four airport sites, 1950-1980 8

7. Coal consumption in New York City in 1887, by area in city: (a) anthracite; (b) bituminous. Coal consumption in New York City in 1909, by consuming sector: (c) anthracite; (d) bituminous coal 10

8. SO_2 emission density for the New York City metropolitan area 11

9. Trend of bituminous coal consumption in the tristate area, 1890-1981 12

10. Estimated trend of residual fuel oil consumption in the tristate area, 1917-1981 13

11. Emission regions of eastern North America 14

12. Sulfur emission trends by geographic regions indicated in Figure 11 15

13. Interpolated wind vectors for the morning and evening sounding of upper air winds 18

14. a) Time-height history for five particles. b) Trajectories of a 100 particle puff subjected to wind veer, shear, and vertical mixing 18

15. a) SO_2 conversion rate constant history for two selected particles. b) S budget for a low level source emitted at 1800 LST. c) S budget for tall stack source emitted at 1800 LST 20

16. a) Deposition field for a surface source. b) Deposition for a tall stack source at St. Louis. For January, tall and short stack source have similar deposition pattern. For July, the tall stack emissions spread further 21

17. Cumulative dry + wet deposition from tall and short stack source. Only for summer emissions from a short stack is the transport distance significantly reduced 23

18. Source attribution of dry + wet deposition at the Adirondacks. a) Emission density for 1978. b) Unit transfer matrix. c) Source attribution map 24

19. Regional model grids used for New York City area SO_x estimates. Numbers indicate SO_x emission densities for area sources (top) and for point sources (bottom) 25

20. Regional model estimates of SO_2 concentration trend in the New York City area.....26

21. Reconciliation of measured SO_2 and b_{ext} with regional model SO_2 concentration.....27

22. Comparison of regional model estimates for New York City area SO_2 concentration and S wet deposition.....28

LIST OF TABLES

1. Summary of CAPITA Regional Model.....16

ACKNOWLEDGEMENTS

This Project was supported by funds provided by Task Group G, Effects on Materials and Cultural Resources, of the National Acidic Precipitation Assessment Program through the United States Environmental Protection Agency. The support of this Agency is gratefully acknowledged as is the advice and guidance of Mr. J.W. Spence who served as Project Officer.

1. INTRODUCTION

All materials deteriorate with time due to natural weathering. However, man-induced chemicals in the ambient atmosphere, most noticeably sulfur dioxide, tend to accelerate this weathering process. For chemically reactive materials, including some metals, there is a measurable weathering rate after a few years of exposure to a polluted atmosphere. Other, more weather resistant materials show a measurable deterioration rate only after atmospheric exposures over a decade or century. Marble falls into the latter category, for which reason it has been used extensively for building exteriors and for monuments.

The marble weathering rate is a measurable quantity, but such data do not reveal the cause of the material's loss nor the apportionment of the loss rate between natural and man-induced causes. For this purpose, estimates are necessary of the environmental history of the exposed material. This includes standard meteorological parameters such as rainfall, frost frequency, temperature, etc. More importantly, for the estimation of the man-induced damage, the concentration history of air pollutants is required. However, quantitative estimates of air pollutant concentrations spanning this century are currently not available.

The quantitative estimation of the specific role of each meteorological and pollutant parameter in marble weathering is a formidable task. The purpose of this modest investigation is to estimate the ambient concentration effects of SO_2 for two sites in the greater New York City area, one with high and another with lower SO_2 concentration history, and to compare the marble loss rate at the two sites Cypress Hills and Long Island. Choosing geographically close locations effectively eliminates the natural weathering as a significant variable, as well as regional scale air pollution influence. Hence, in this case the differences in the weathering rates are reasonably attributable to the man-induced local air pollution. The marble loss rates and the estimated SO_2 concentration histories at the two sites permit a crude estimate of the damage function, i.e. loss rate increase per SO_2 concentration increase.

The current investigation of tombstone weathering rates is broken down into two parts: (1) Retrospective reconstruction of the chemical environment (SO_2 concentration and SO_4 wet deposition); (2) Marble loss rate as a function of SO_2 concentration. The present report is devoted to part 1.

2. METHODOLOGY FOR RETROSPECTIVE AIR POLLUTION ANALYSIS

This section outlines the methodology used for the reconstruction of the atmospheric chemical environment. At this stage, the method is not specific to any atmospheric chemical substance or environmental effect. The method will be applied specifically to the sulfur oxide reconstruction over the New York City area for the purpose of material damage estimates.

For purposes of analysis, we adopt the convention that the spatial scale below 100 km is called local, while beyond this distance lies the regional scale. The local and regional models cover the corresponding spatial scales. At any given location, the concentrations and depositions are a combination of nearby (less than 100 km from receptor) and distant sources.

Reconstructing the chemical history for a given location requires at least five distinct steps:

1. **Gathering of data on pollutant concentrations.** Such data are generally sparse in time and space, but provide significant anchor points for the reconstruction.

2. **Reconstruction of emission trends.** In general, it cannot be stated a *priori* which

is the region where the emission trends need to be reconstructed. This is due to the fact that the region of influence of each source depends strongly upon the pollutant of concern. For example, the surface concentration of sulfur dioxide is mostly influenced by local sources; sulfate aerosol and sulfur wet deposition are determined by the regional source distribution.

3. **Regional background concentrations and depositions.** The contribution of sources to the regional background can be calculated via a long range transport model, along with suitable regional emission inventories. We are not aware of alternatives to this approach.

4. **Local concentrations.** The sulfur dioxide concentration is strongly influenced by sources on the local scale (100 km), requiring a local emission inventory and a local scale dispersion model. Alternatively, the existing monitoring data may be used to develop the local concentration field.

5. **Reconciliation of monitoring data with model estimates.** This is the feedback stage where the model parameters are explored and modified to better match the observations.

A unifying tool used for all of the above stated tasks is that of pollutant flow accounting. This method is explained below in more detail.

The flow of matter from the producers to consumers and subsequently to the receptors is depicted schematically in Figure 1. Most of the "production" of potential pollutants initiates by mining, that is removal of a substance from its long term geochemical reservoir. The amount of pollutant mass, M_i, that is mobilized by mining is the production rate P_i of the raw material (coal, oil, smelting ore, etc.) multiplied by the concentration c_i of the impurity (sulfur, mercury, lead, etc.), $M_i = c_i\ P_i$.

The transfer of matter from the producer to the consumer occurs by ground transportation, including railroad, trucks, barges, etc. Functionally, the surface transport redistributes the mined substances over a large geographical area. In principle, every producer, i, may deliver its product to any consumer, j. Numerically, this producer–consumer transfer is characterized by a surface transfer matrix, s_{ij}.

The amount of matter that is used at consumer j that originates from producer i is $U_{ij} = s_{ij}\ M_i$. The total amount of matter reaching the consumer j is the sum of the matter produced by all producers multiplied by their respective surface transfer matrix elements.

The next transfer occurs between the consumer and the receptor. The consumer is defined as the location where the combustion or smelting occurs. The receptor, in turn, is the location where the pollutant is deposited following its atmospheric transit. Again, in principle all consumers j can transfer matter through the atmosphere to all receptors k. Hence, the matter received at receptor k that originated at consumer (emitter) j, R_{jk}, is the product of the use rate U_j times the atmospheric transfer matrix from emitter j to receptor k: $R_{jk} = a_{jk}\ U_j$. The total amount of matter deposited at receptor k is the sum of the use rates U_j at each emitter weighed by its atmospheric transfer matrix element to receptor k, a_{jk}.

It is thus apparent that in order to account for the flow of matter from the producers to the receivers one needs to acquire information about four sets of parameters: the production rate of raw matter, the concentration of impurity (e.g. sulfur content), the surface transfer matrix, and the atmospheric transfer matrix. The numeric values of these coefficients and matrix elements are discussed in detail in Husar,1985, NAS report, with emphasis on sulfur.

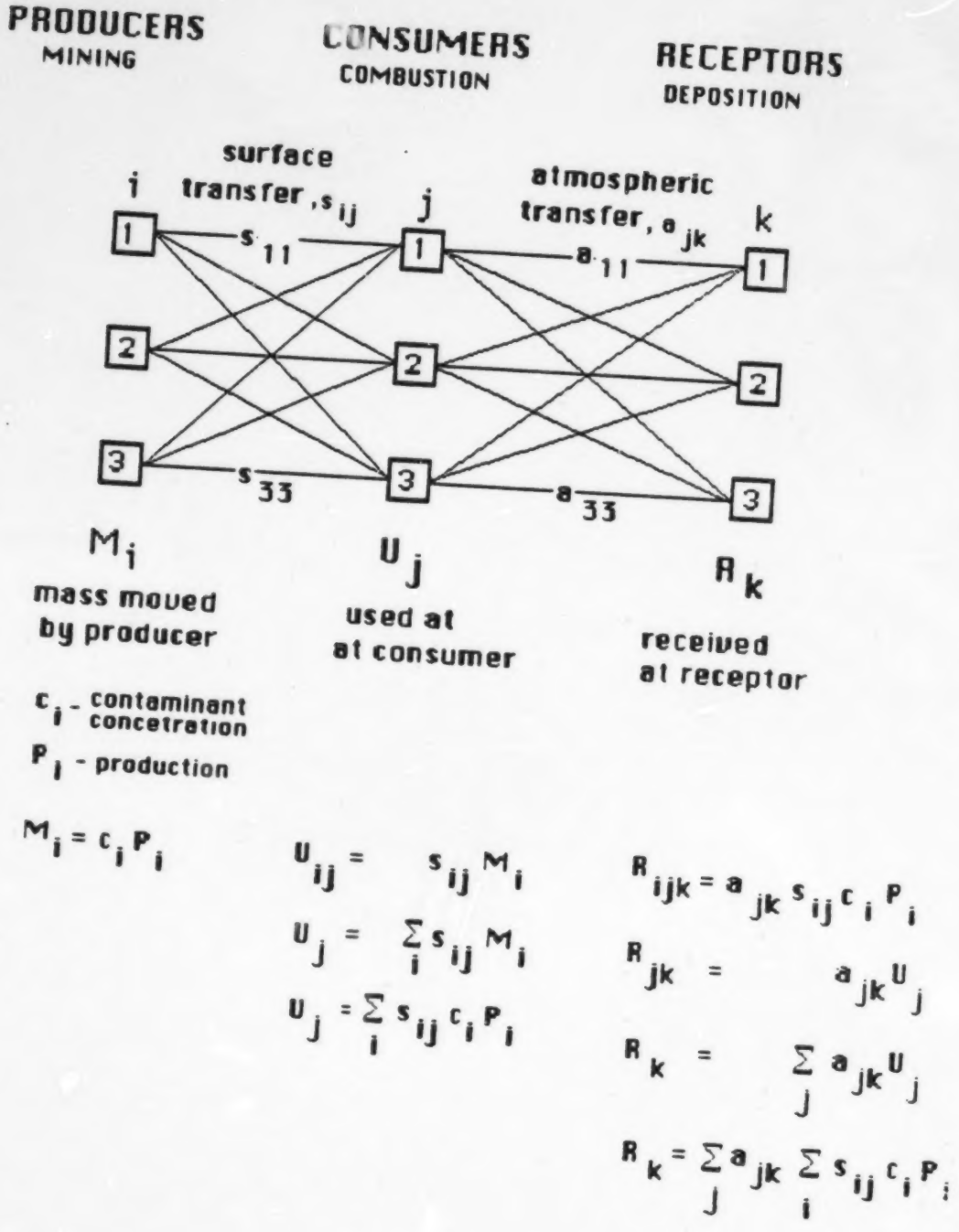

Figure 1. Schematic illustration of the mass balance approach to pollutant flow.

3. AMBIENT CONCENTRATIONS OF SULFUR COMPOUNDS

The air pollution in New York City has had a dynamic past. Not only the amounts of polluting substances but their mix has changed remarkably in the course of this century. The retrospective SO_2 concentration estimates discussed below are based on a historical reconstruction of the S emission trends for the greater New York City area. The assumption is made that the concentration fields were similar in shape (but not in magnitude) to the measured values in the late 1960s. The crucial assumption here is that the source distribution within the metropolitan area has not changed so as to significantly alter the concentration ratio at the two sites since the turn of the century.

The concentration and deposition of sulfur compounds at the two receptor sites, Cypress Hills and Long Island, are determined by the spatial- temporal distribution of the SO_2 emission field and the atmospheric ventilation surrounding the two sites. The historical concentrations at these two sites may be estimated directly from measurements or from a suitable retrospective air quality model. The available SO_2 and sulfate concentration data are limited in spatial and temporal coverage. On the other hand, numerical source- receptor models are also limited by their own severe uncertainties. The following reconstruction is guided by both existing monitoring data as well as by model estimates.

SO_2 concentration measurements

Sulfur dioxide concentrations have been measured at a few locations and for short time periods, dating prior to World War II. However, considering the limited spatial and temporal coverage, such data cannot be meaningfully applied for the present purpose. More extensive day by day sampling and analysis of New York air began in 1953. The sampling sites included Manhattan, Queens, Brooklyn, the Bronx, and Staten Island. The data were summarized by W. O. Negherbon (Edison Electric Institute, Research Project RP62, June 1966). Another summary of the SO_2 concentration trends was reported by Blade and Ferrand (1969). More recently, Eisenbud et al. (1973) gave an updated summary of the SO_2 concentration data for Nassau and Suffolk counties. We have used the SO_2 data in the above references to assemble a 15 year trend for the New York City Central Park, 1958-1972. The trend data shown in Figure 2 indicate about 0.12 ppm around 1960, rising to over 0.20 ppm in 1965, followed by a sharp drop in the late 1960s. It is presumed that the concentration reductions continued in the 1970s.

The pattern of SO_2 concentration surrounding New York City is shown in Figure 3a and 3b, for January 1969 and July 1970, as reported by Eisenbud et al. (1973). It is evident that the highest concentrations have been measured on Manhattan and adjacent sectors of Brooklyn, Queens and the Bronx. The gradient is particularly pronounced for the winter season, when Manhattan concentrations exceed 0.2 ppm while the concentrations 30 miles away on Long Island are below 0.05 ppm. Based on the above maps, we estimate that the SO_2 concentration at the Cypress Hills site is about 60% $\pm$ 20% of the Central Park readings, while the Long Island site is 30% $\pm$ 20% of the Central Park concentration.

The concentration field is variable over three characteristic time scales: diurnal, seasonal and secular. The diurnal emission trends are reflected in SO_2 concentration data for New York City, 1954, as shown in Figure 4. For the winter season, there is a peak between 6 and 10 AM, and another at 6 to 10 PM. Undoubtedly, the diurnal pattern is influenced by the emissions as well as by the horizontal and vertical ventilation. The seasonal SO_2 concentration trend is shown in Figure 5, indicating a factor of two higher wintertime SO_2 concentrations compared to the summer values.

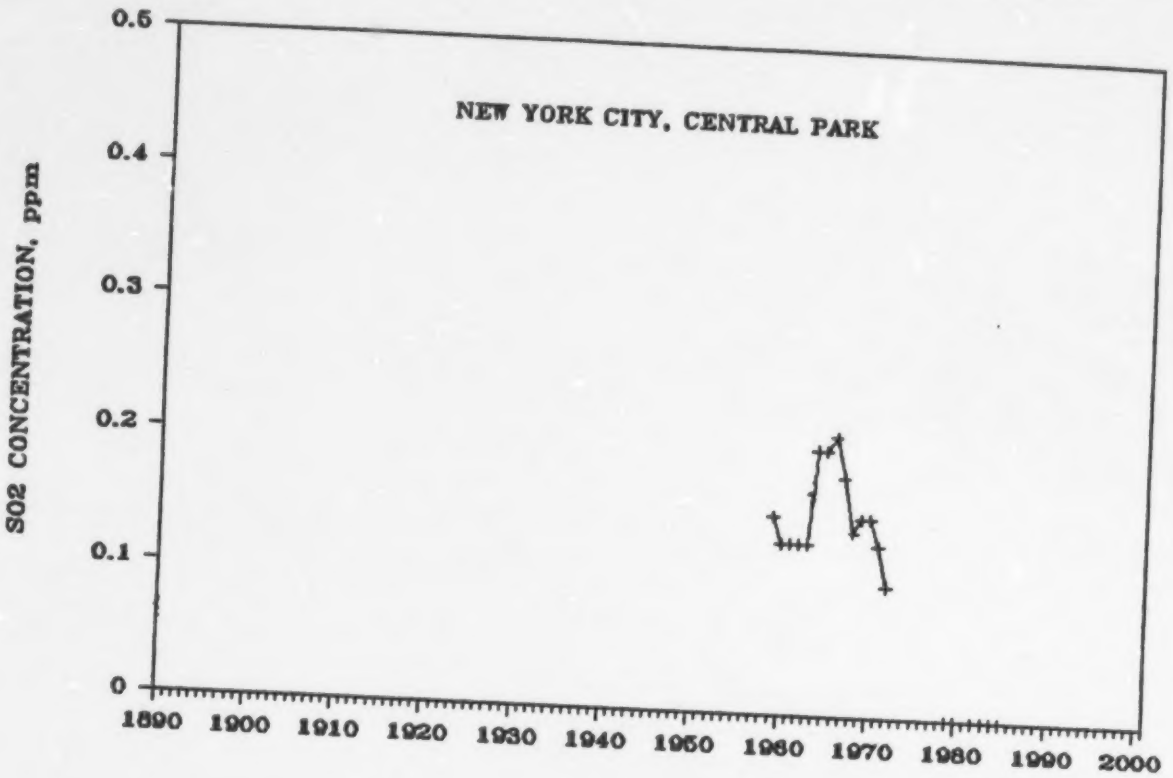

Figure 2. Fifteen year trend of sulfur dioxide concentration in Central Park, adopted from Eisenbud et. al. (1973)

Haziness

The most noticeable index of atmospheric pollution is haziness, i.e. the reduction of visual range. Atmospheric haze in urban areas arises from a mix of optically active fine particles. Changes in emission pattern of manmade fine particles, or their precursor gases, are reflected in changes of haziness.

Haziness is monitored routinely by human observation of visual range. The measure of haziness is the extinction coefficient, b_{ext}, defined as $b_{ext} = k$ / visual range, where k=24 if visual range is expressed in miles. The extinction coefficient has units of km^{-1}, and is proportional to the concentration of light scattering and absorbing fine particles. In what follows, haziness trends are expressed in terms of mean extinction coefficient derived from visual range observations. Only daytime observations in the absence of fog and precipitation are considered. The trend of haziness is shown for four airports in the New York City area: LaGuardia, Newark, JFK, and Providence RI (Figure 6). Winter observations are shown (Jan.,Feb., March) to emphasize the relative trends among the stations. The summer observations, not shown here, did not exhibit substantial variation among the four stations. For the 1950-1980 time period, the highest haziness was reported for LaGuardia, which peaked around 1960. Next in haziness were Newark, JFK, and Providence. The first three airports show much higher winter haziness in the 1950s than in the 1980s. On the other hand, Providence shows no substantial trend over the 30 year period. It is remarkable to note that by 1980 all four airports have haziness within 20%, Providence showing the highest values.

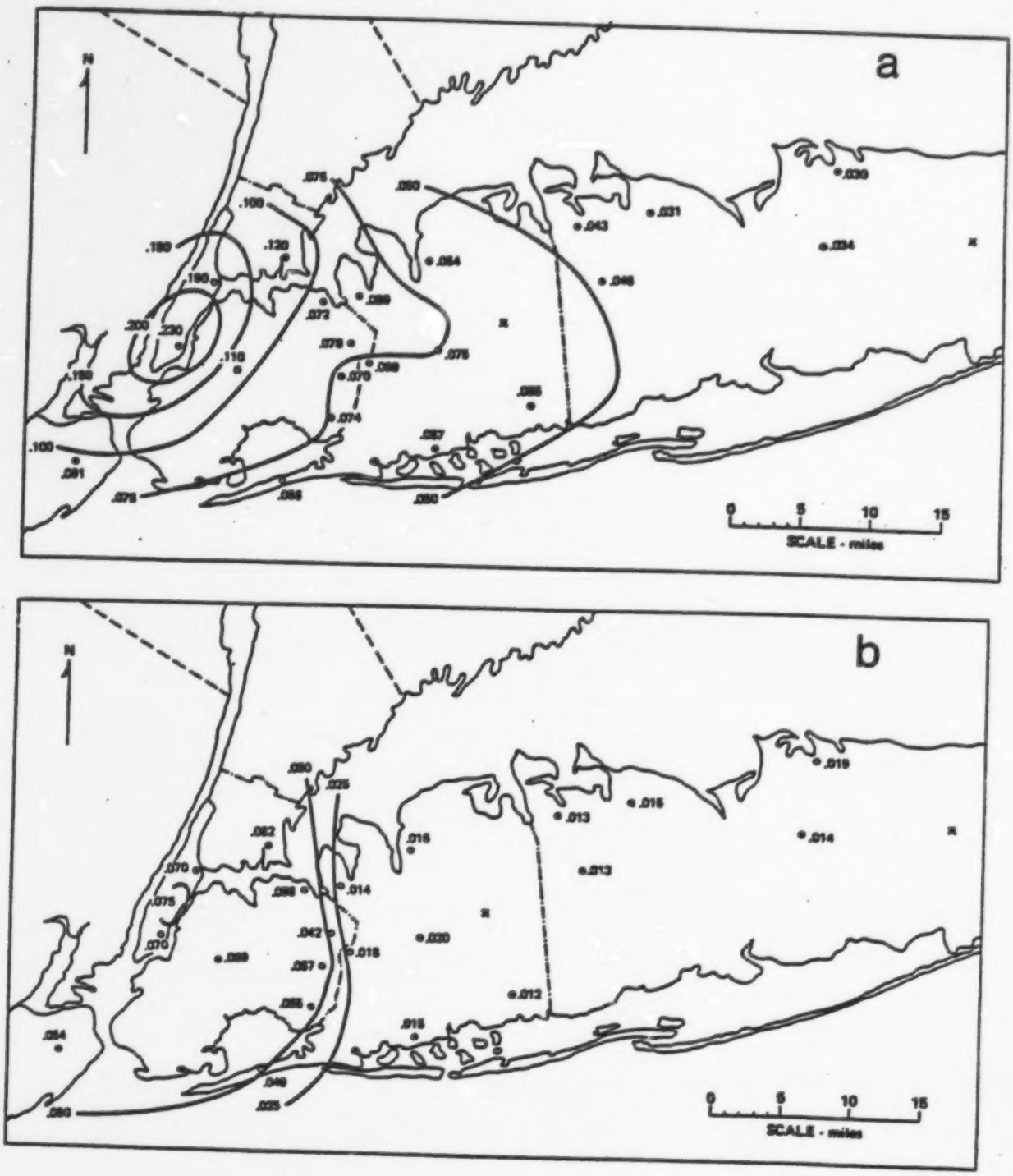

Figure 3. Observed SO_2 concentration fields for the New York City area from Eisenbud, et. al.,(a) January, 1969; (b) July, 1970.

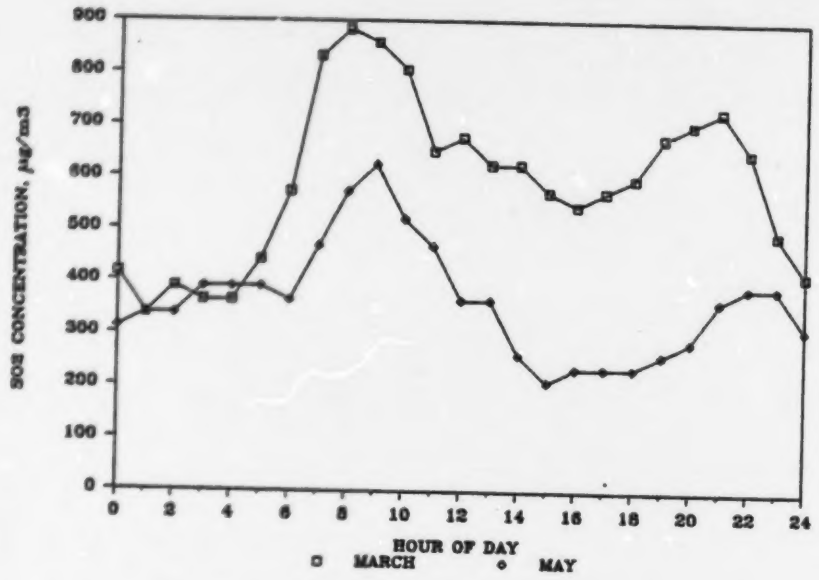

Figure 4. Diurnal SO_2 concentration for New York City, 1957-1967.

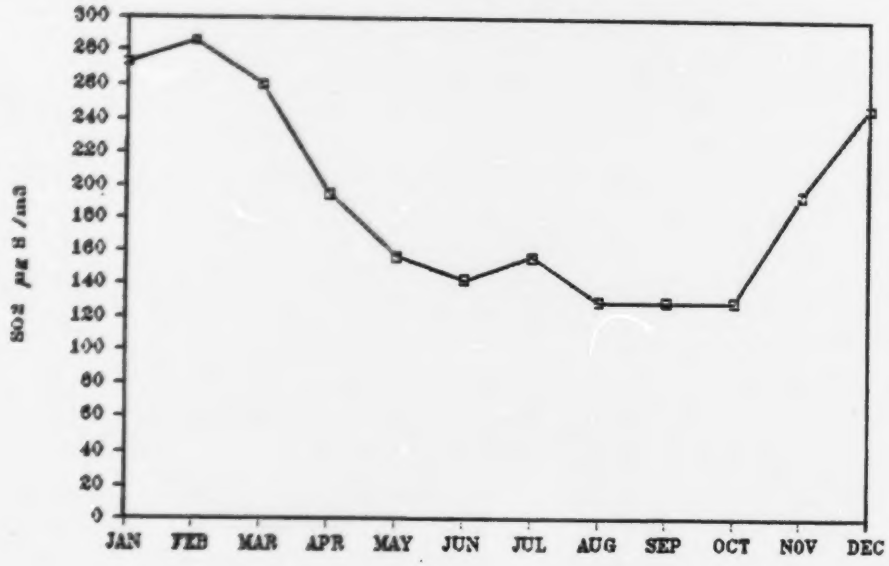

Figure 5. Seasonal SO_2 concentration for New York City, 1957-1967.

Recognizing that the visual range observations do not necessarily reflect trends in sulfur

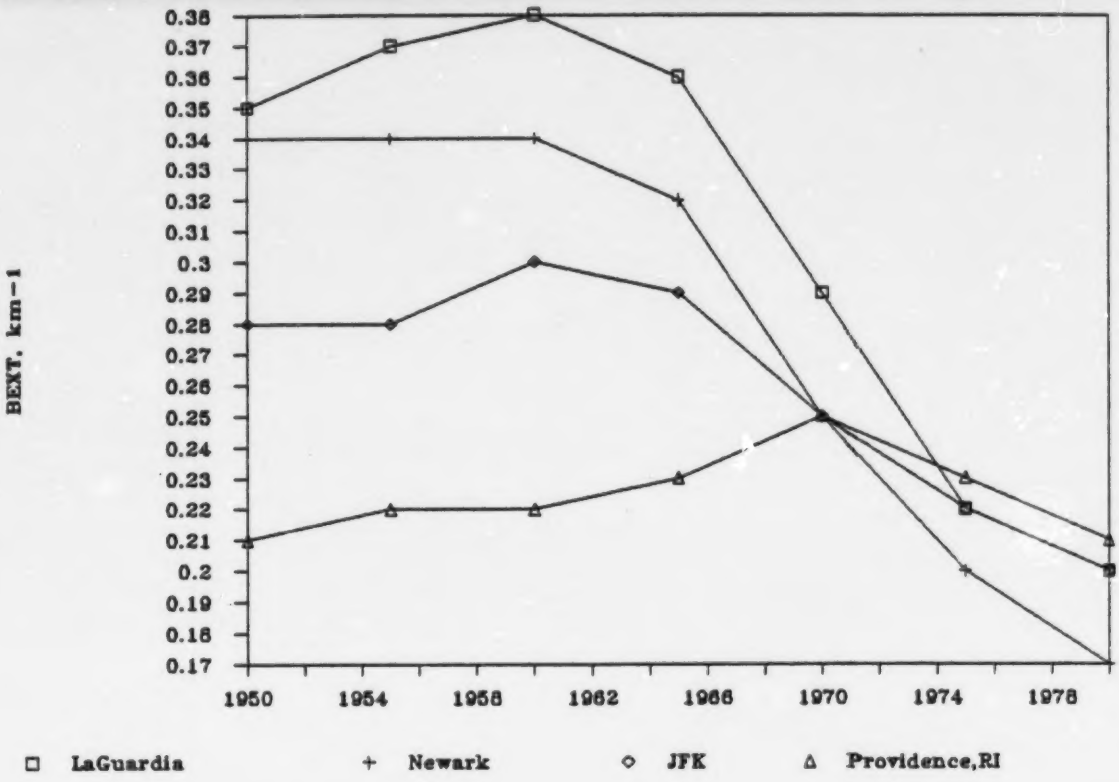

Figure 6. Trend of winter quarter haziness at four airport sites, 1950-1980.

dioxide or sulfate aerosol, it is nevertheless likely that the drop in haziness also reflects a drop in general pollution levels of SO_x over the years 1960-1980.

Summarizing the ambient monitoring data for SO_2, SO_4 aerosol, and haziness, it may be stated that the concentrations in the 1950s were substantially higher than in the 1970s. Furthermore, the haze data indicate that the pronounced high concentration gradients of the 1950s have been reduced; hence, there has been a substantial regionalization of air pollution. Currently, the urban-industrial centers exhibit only a slight perturbation above the regional background.

4. SULFUR EMISSION TRENDS AFFECTING THE NEW YORK AREA

Essentially all manmade air pollution over the eastern U.S. results from the combustion of fossil fuels. Prior to the 1950s, coal was the dominant source of energy for all economic sectors, and coal was also responsible for most of the air pollution. Oil products became significant only since the 1950s. Smelting of metals has not been a significant factor in air pollution over the industrialized Northeast.

New York area trends

The reconstruction of the sulfur emission trends is based on the fuel consumption data and on the estimate of the sulfur content of the pertinent fuels. In the following, the historical emissions for the New York City metropolitan area are reconstructed based on the consumption of anthracite, bituminous coal and residual fuel oil.

Around the turn of the century, New York City and its vicinity was the metropolitan area with the largest population in North America. Its energy needs were satisfied by coal imported from surrounding states (PA,WV and MD). During those years, Pennsylvania anthracite was still in abundant supply and that fuel was used rather than bituminous coal to conform to the contemporary antismoke ordinances. In particular, residential homes, hotels, large office buildings and apartment houses and their central heating plants were fueled by anthracite.

The first data set which we have uncovered for fuel consumption in the New York City metropolitan area dates back to 1887 (Mineral Resources of the U.S., 1887). The total coal consumption was 8.1 million tons, of which 5.7 million was anthracite and 2.3 million was bituminous coal. New York City itself (64%) and Brooklyn (26%) accounted for the bulk of the anthracite consumption. For bituminous coal, these two regions were even more significant, as depicted in the pie charts of Figs. 7a,b.

The quantity of coal consumed in the New York City area in 1909 has been estimated by R.W. Morris and reported in Mineral Resources Yearbook. Anthracite consumption amounted to 11.4 million tons, while bituminous coal use was only 4.3 million tons. The breakdown of anthracite use by consuming sectors is given in the pie chart of Figure 7c,d. Evidently domestic consumption,offices and hotels accounted for 70% of the total. Bituminous coal consumption, on the other hand, was dominated by factories (42%) and utilities (37%). Morris points out that bituminous coal consumption was allowed if proper smoke emission controls were taken. He also stated that the ordinances were not strictly enforced, especially in the case of large powerhouses on the riverfront.

The coal supplies to the New York City area came from the Clear Field and Broad Top regions in central Pennsylvania, from Cumberland and Georges Creek regions in Maryland, and from some districts in western Pennsylvania.

The SO_2 emission density within the metropolitan New York area for recent years is illustrated in Figure 8.

Fuel consumption data with the above detail are not available to us for other years. Extrapolation to other periods requires the use of other more general data sets. The above data sets constitute anchor points around which the fuel consumption data were estimated.

The yearly coal consumption data were reported in the yearbooks "Mineral Resources of the U.S.", from which the state by state consumption can be estimated. We have used the data from the yearbooks for the one year/state resolution for the time period 1889-1959. The fuel consumption data for the 1960-1981 period were obtained from the U.S. DOE(1983). The bituminous coal demand of the New York City area in 1909 was 4.3 million tons, while in the surrounding tristate area (New York, New Jersey and Connecticut) the demand was 39 million tons. We assumed that the New York City metropolitan area has consumed the same fraction of the tristate consumption for the past 100 years. We recognize that there may have been subregional shifts in the tristate coal consumption, but we are not in position to quantify such spatial trends. It was assumed that the New York City metropolitan area consumed 11.5% of the tristate bituminous coal consumption. The consumption of bituminous coal in three states surrounding the New York metropolitan area is depicted in Figure 9. It is evident that there has been a steady rise in the demand from the late 1800s through 1915, followed by 15 years of stagnation. Starting in 1930, the Great Depression caused a significant drop in the coal demand, followed by a second peak during World War II. In the 1950s, the coal use dropped again to the levels of the depression years. The most significant drop, however, started in 1968, resulting in coal demand for the 1970s that is similar to that at the turn of the century.

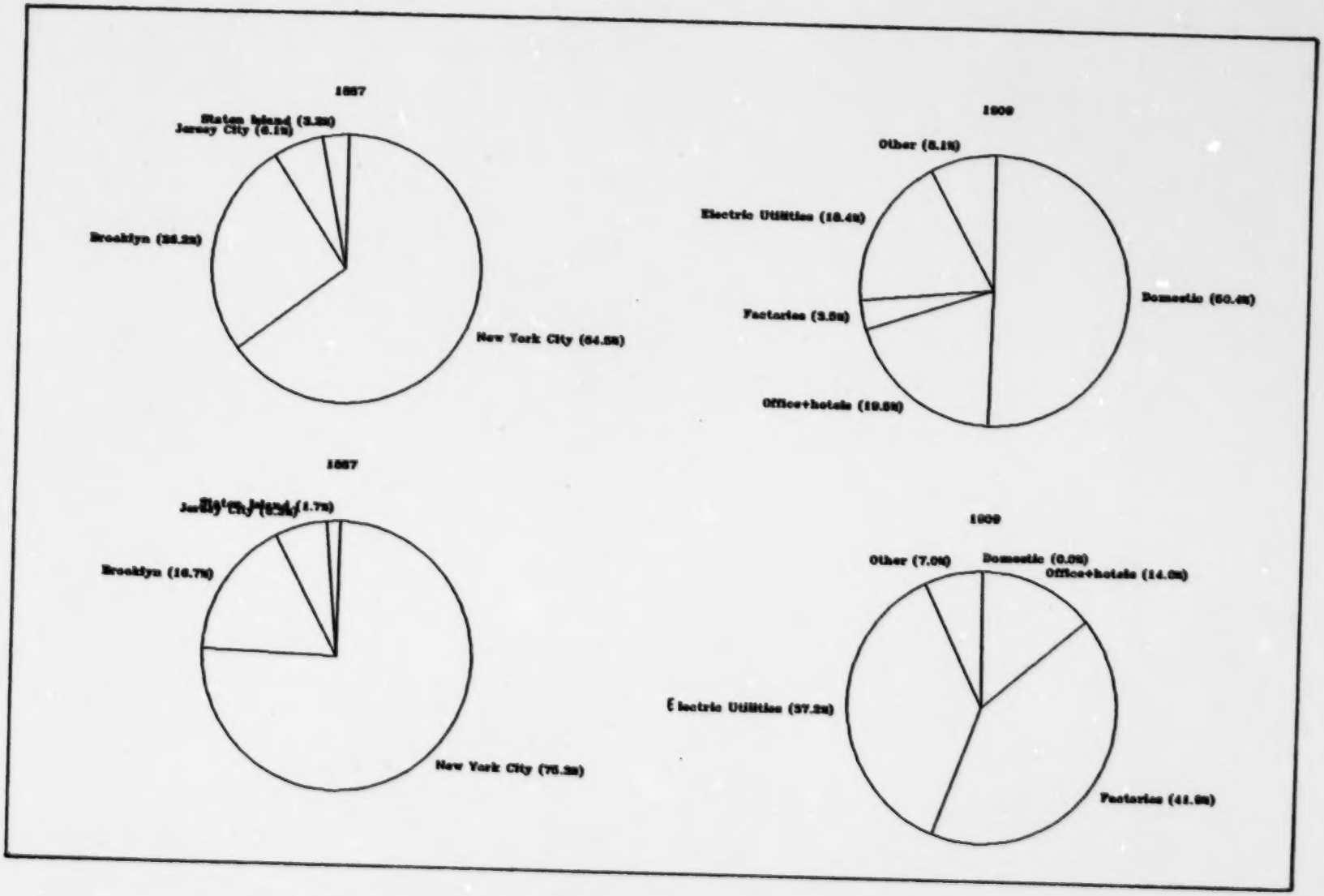

Figure 7. Coal consumption in New York City in 1887, by area in city: (a) anthracite, top; (b) bituminous, bottom. Coal consumption in New York City in 1909, by consuming sector: (c) anthracite, top; (d) bituminous, bottom.

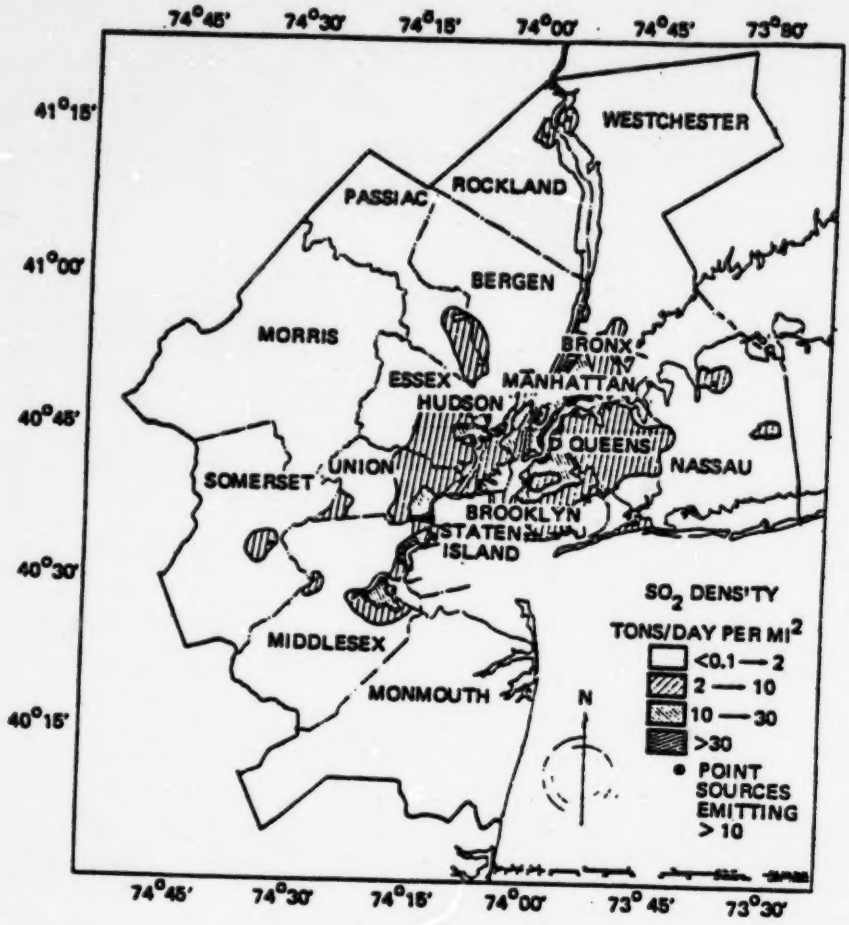

Figure 8. SO_2 emission density for the New York City metropolitan area.

Volatile distillates of crude oil, including gasoline and distillate fuel oil, do not contain significant amount of sulfur. However, residual fuel oil contains significant sulfur in amounts that strongly depend on the origin of the crude. Some crudes contain several % sulfur by weight, others only a few tenths of percent. For the years 1960-1981 the residual fuel oil data was taken from the DOE database(1983). For the time period prior to 1960, the New York City area consumption was scaled to the national residual fuel oil consumption reported in the "Historical Statistics of the United States. Colonial Times to 1970." The resulting estimate for the residual fuel oil consumption trend is shown in Figure 10. It is evident that there has been an overall increase since the turn of the century to about 1970, followed by a strong decline since 1970. In fact, we estimate that the 1981 residual fuel oil consumption is comparable to the demand in the 1920s.

The above discussion of the emissions in the vicinity of New York City are given to illustrate the general pattern. However, these data will not be used other than through incorporation into the regional model.

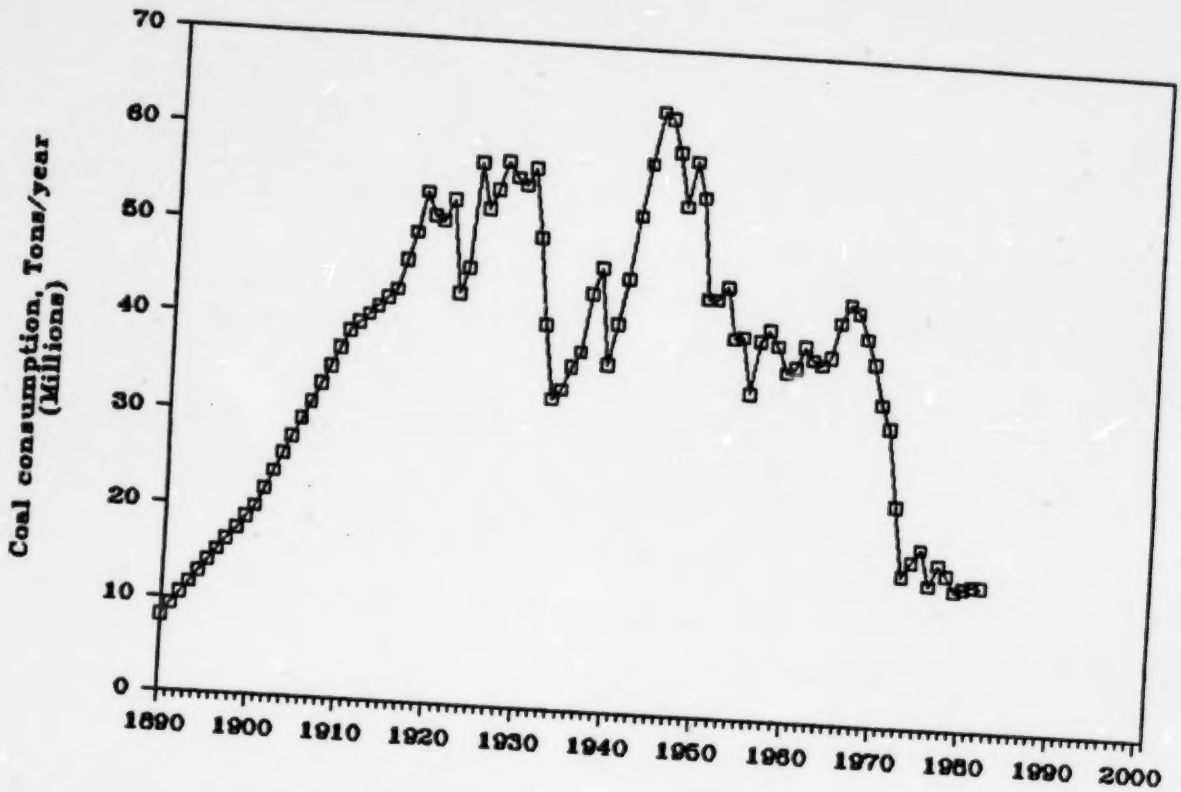

Figure 9. Trend of bituminous coal consumption in the tristate area, (NY,NJ,CT) 1890-1981.

Eastern North American trends

In order to estimate the contribution of regional sources to the New York City area, consideration needs to be given to the emission trends over large parts of eastern North America.

This section summarizes the sulfur emission trends for eastern North America. These include eastern U.S. and eastern Canadian sulfur emissions from coal and oil combustion, as well as copper and zinc smelting. The eastern Canadian emission trends were taken from the U.S.-Canadian Memorandum of Intent reports and were extrapolated for pre-1955 years using Canadian smelter production data. More detailed discussion of the sulfur emission trends may be found in Husar, 1985, NAS report.

The sulfur emission trend for eastern North America is shown in Figure 12a. The two lines indicate high and low estimates. Emission estimates are presented in this manner to encourage the reader to incorporate uncertainty in interpretation of these results. The sulfur emissions show a wavy upward trend since 1880, with peaks in 1920s ,1940s and early 1970s.

For the current period, the sulfur emissions are estimated to range between 11 and 15 million tons/year (22-30 million tons SO_2/year).

There are substantial differences in the emission trends of regions within eastern North America. For this reason the subcontinent was divided into five regions shown in Figure 11.

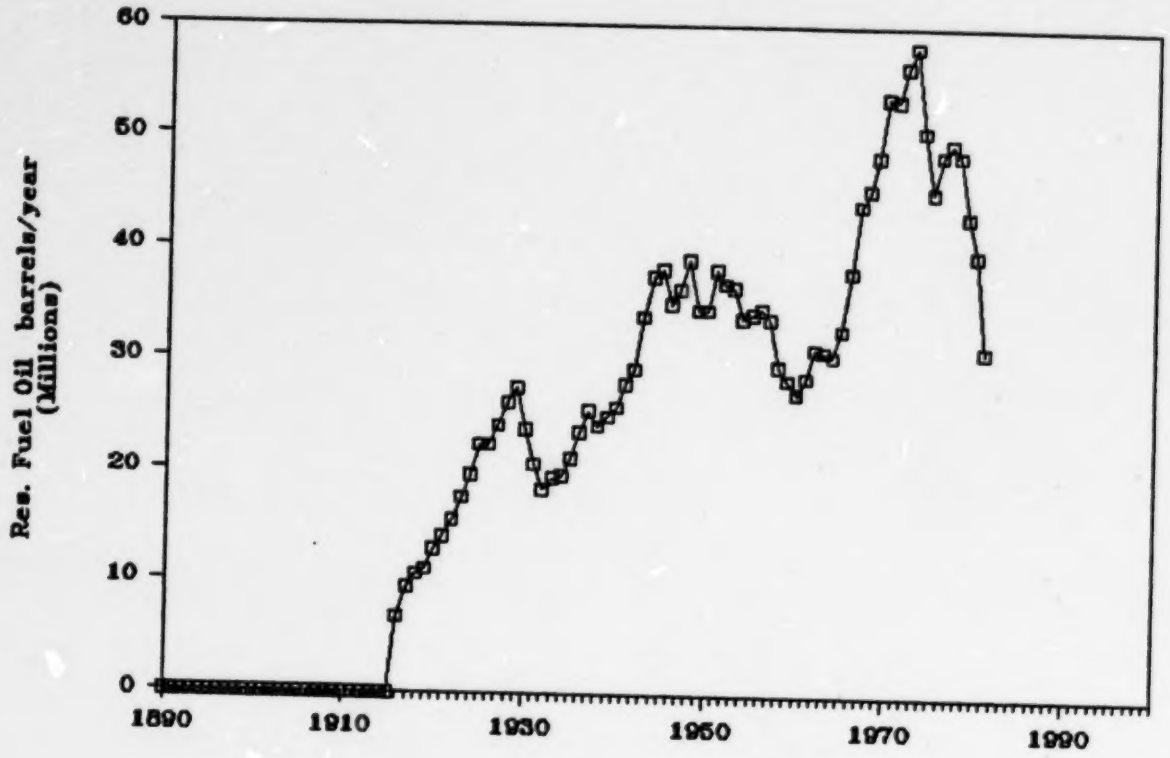

Figure 10. Estimated trend of residual fuel oil consumption in the tristate area, 1917-1981.

The emission trend for eastern Canada Region 1 (Figure 12b) shows an increase since the turn of the century leading to a peak at about 3 million tons in the mid 1960s, followed by a decline since then.

Sulfur emission trend for the northeastern states, including Pennsylvania (Region 2) is given in Figure 12c. The strong increase of emissions began in the 1890s, leading to peak between 1910 and 1930, followed by a depression in the 1930s. Another increase occurred in the 1940s and the emission levels remained roughly constant until the mid 1970s, when another decline occurred. The current SO_x emissions are comparable to those in the 1930s and 1910s but substantially below the 1920s, 1940s and 1960s.

The emission trend for the eastern states south of the Ohio River is given in Figure 12d. The emissions were low in the southeastern U.S. until about 1960, when a strong increase occurred. This upward emission trend persisted into the 1980s.

Sulfur emission trend for the industrialized midwest, including Illinois, Indiana, Michigan, Missouri, and Ohio is given in Figure 12e. The emission trend in this region shows a doubling since the turn of the century, with peaks in the 1920s, 1940s, and 1980s and depressions in the 1930s and 1950s.

Sulfur emission trend for the upper midwest, Iowa, Minnesota, Wisconsin is given in Figure 12f. The emissions in this region were low in the early part of this century, and remained at low

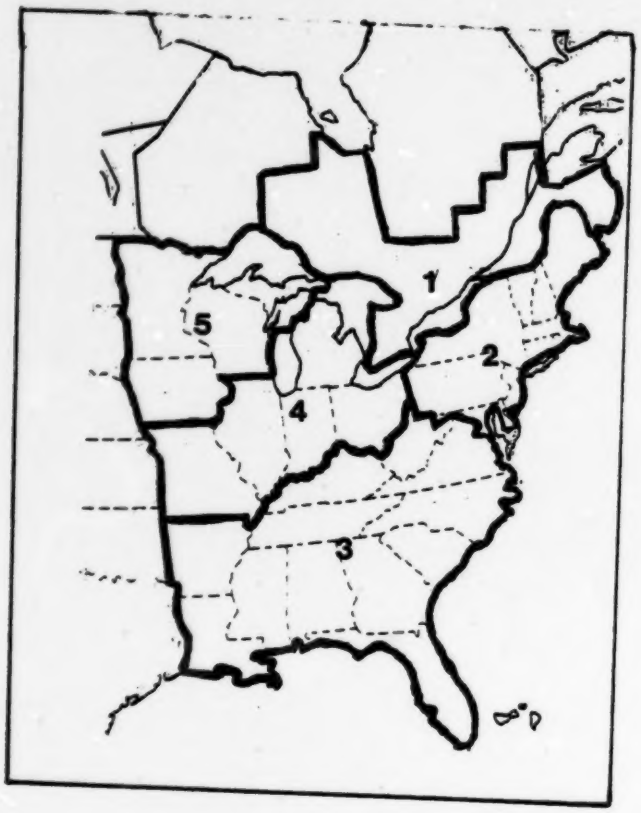

Figure 11. Emission regions of eastern North America.

levels until the 1980s.

Comparison of the sulfur emissions north and south of the Ohio River shows that the emissions north of the Ohio River (Regions 1,2,4, and 5) have increased about 25% since the 1920s. In contrast, the emissions south of the Ohio River (Region 3) show a threefold increase since the 1930s. Currently, the sulfur emission density is comparable for the regions north and south of the Ohio River.

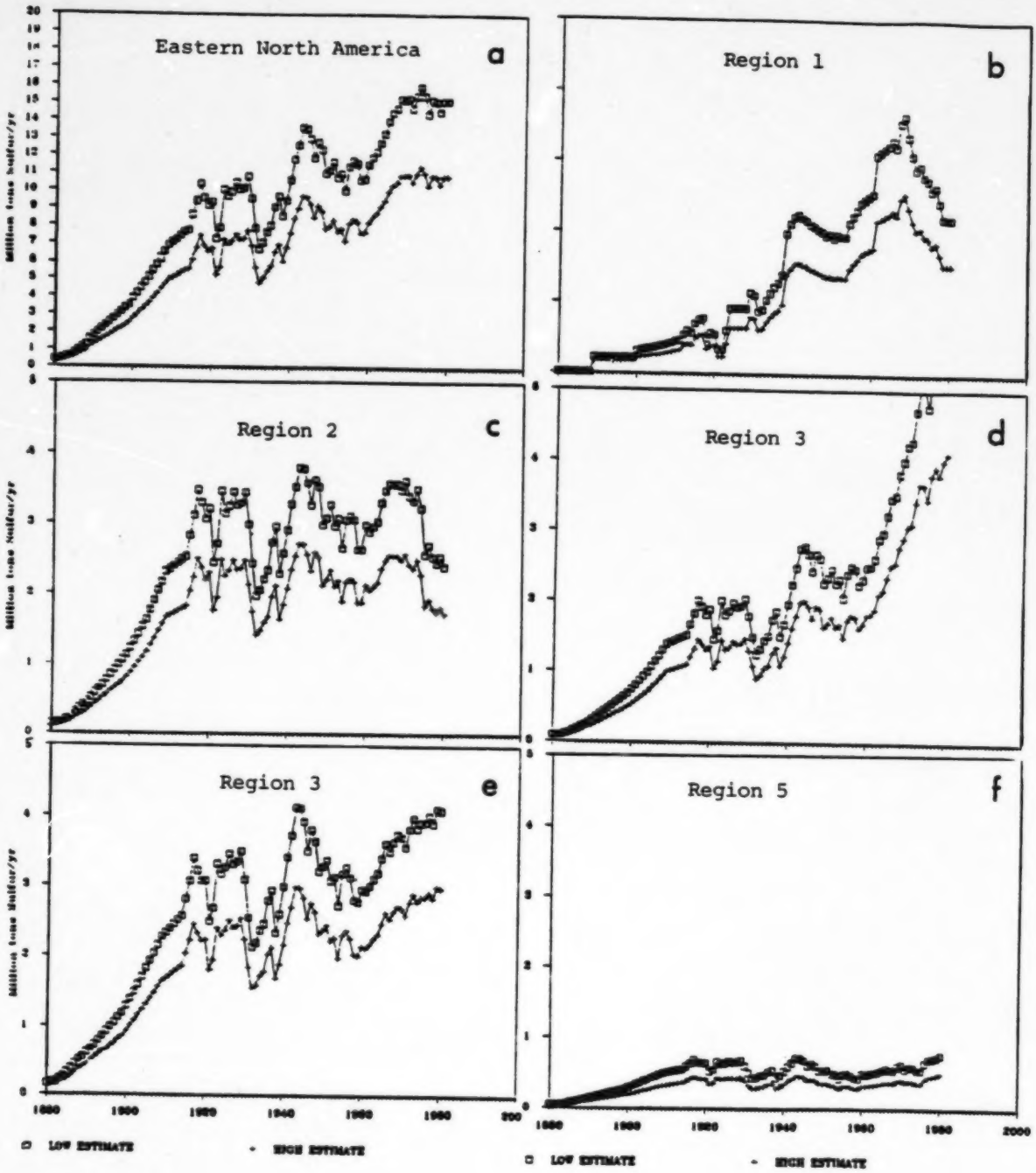

Figure 12. Sulfur emission trends by geographic regions indicated in Figure 11.

5. REGIONAL MODEL

A long range transport model is used for the regional background estimate. We are applying a Monte Carlo or direct simulation scheme for the dispersion, transformation and deposition of individual puffs of pollutant. The initial model development was reported by Patterson et al., 1981. Further details of the current model are described by Patterson et al., 1985. The discussion of our local model in the following section also provides illustration of many features of the regional simulation.

The regional model formulation is summarized in Table 1.

TABLE 1. SUMMARY OF CAPITA REGIONAL MODEL

a. Model Type	Monte Carlo (Lagrangian, and Eulerian in the limit of large number of quanta)
b. Receptor Grid Resolution	52 x 60 grids 127 x 127 km at 60 degrees north latitude (one-third of U.S. National Meteorological Center grid spacing)
c. Model Domain	North America
d. Model Output	Fields of particles each 3-h, each particle representing a mass of emitted pollutant remaining in the atmosphere as each possible chemical species; converted to fields of daily SO_2, SO_4 concentrations and dry and wet depositions in each grid
e. Input Requirements	
Emissions	Seasonal, surface and tall stack 1890-1980 SO_2 grids
Winds	0000 and 1200 GMT rawinsonde wind profiles at 130 sites
Precipitation	3-hourly observations of precipitation of three intensities at surface synoptic sites
Cloud cover	gridded from 3h surface synoptic sites
Mix heights	Climatological by season, from work of Holzworth(1972) and Portelli(1977), of maximum afternoon mixing heights.
f. Emissions	3-h SO_2 emissions. Released in mixed layer in day, and either 150-450 layer or 0-150m at night; 1% primary SO_4
g. Transport	Inverse-distance squared weighting. Upper air rawinsonde winds are interpolated in space into 11 layers (0-150, 150-450,450-750,750-1050,1050-1350,1350-1650, 1650-1950,1950-2250,2250-2850,2850-3450, 3450-5250 m above ground) Wind for each layer is the vector average,

	and winds are linearly interpolated from 12h to 3h, using seasonal diurnal interpolation factors at each height to reflect nightime jets and midday drag from convective mixing.
h. Precipitation	3h grids of the space-time average probability of encountering precipitation are used to scale local wet removal rates as fraction of the maximum rate.
i. Mixed Layer	climatological average, which varies with geographic location and season of year. Representative peak P.M. values are 800 (winter), 1200 (spring,fall), 1350 (summer). Fixed 150 m at night.
j. Horizontal Dispersion	lateral displacement by veering of layers overnight; "eddy diffusion" K=2000 m^2/s day,100 m^2/s night.
k. Vertical Dispersion	instantaneously mixed throughout mixed layer during day (0900-1800 LST); no vertical mixing at night.
l. SO_2 Transformation Rate	varies seasonally, diurnally and locally. Proportional to solar radiation, function of latitude/season, time of day, and local total sky cover.
m. Dry Deposition Rate	Zero above local mixed height and above 150m night surface layer. Varies with stomatal density and opening according to solar radiation plus offset.
n. Wet Removal Rate	Zero above local peak afternoon mixing height Within mixing layer: (precipitation probability over a grid during a specified time) x (wet removal rate constant, 100%/h for SO_4 and 30%/h for SO_2, with rates one twelfth in frozen precipitation).

Transport. The wind field for the transport of individual emission quanta is obtained by spatial (location and height) and temporal (time of day) interpolation of U.S. and Canadian rawinsonde wind data obtained twice a day. For each 3 hour time segment, the wind field is gridded for each of the 11 height layers. Two example wind fields for the lowest layer (0-150 m) and 1050-1350 m are in Figure 13. During the nighttime, the emission quanta are transported within a given layer without vertical exchange. During the daytime, the puffs are moved randomly between the layers up to the height of the local climatological mixing height as illustrated in Figure 14. The consequence of the layered nighttime transport followed by random displacement during the day is a displacement of quanta, i.e. synoptic scale dispersion (Figure 14). Superimposed on this wind field driven dispersion is a daytime eddy diffusivity of 2000 m^2/s. Most of the displacement is driven by the inhomogeneities of the measured wind field (wind shear and veer) rather than by the eddy diffusion.

The transport field is assumed to be the same as the wind field in the 1970-1980s. In the transport module, special emphasis is placed on the dispersion simulation of low-level (near

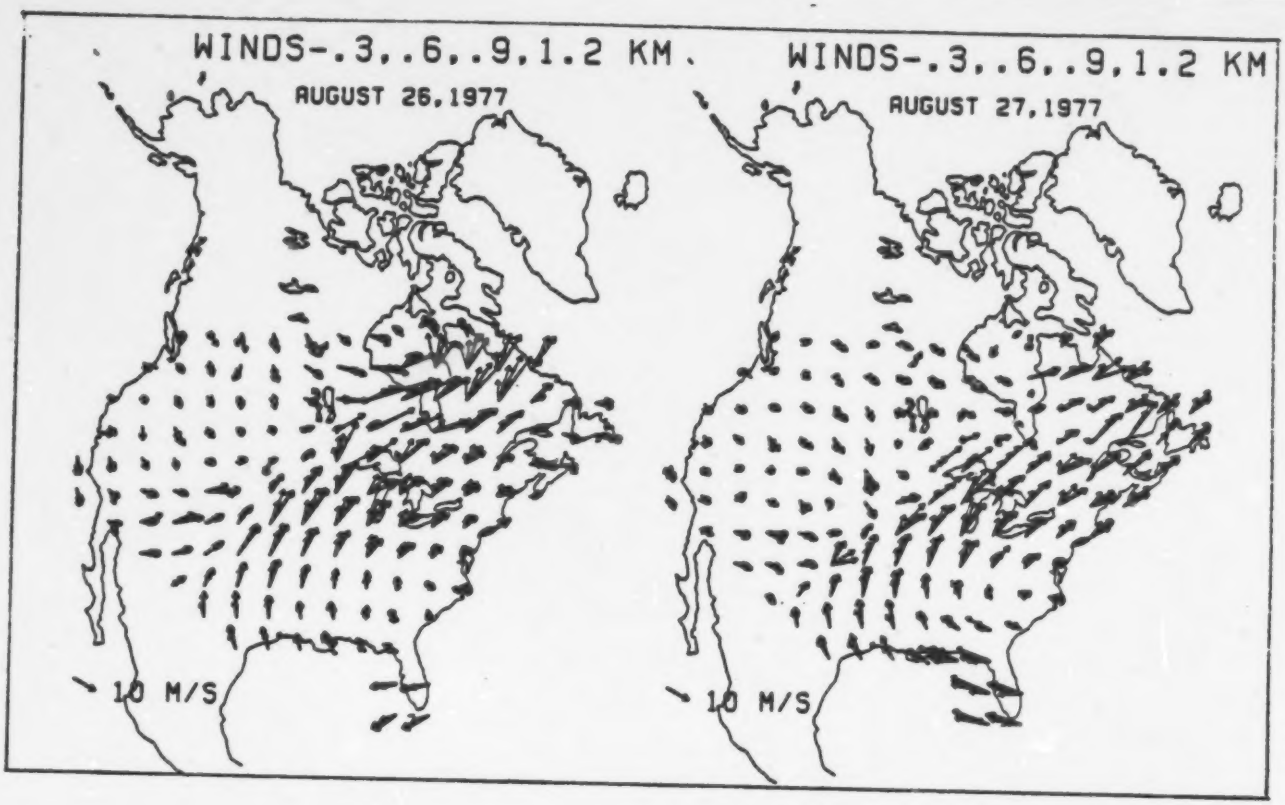

Figure 13. Interpolated wind vectors for the morning (right) and evening (left) sounding of upper air winds. The shortest arrow is the 0-300m average. The longest arrow is at 1 km height.

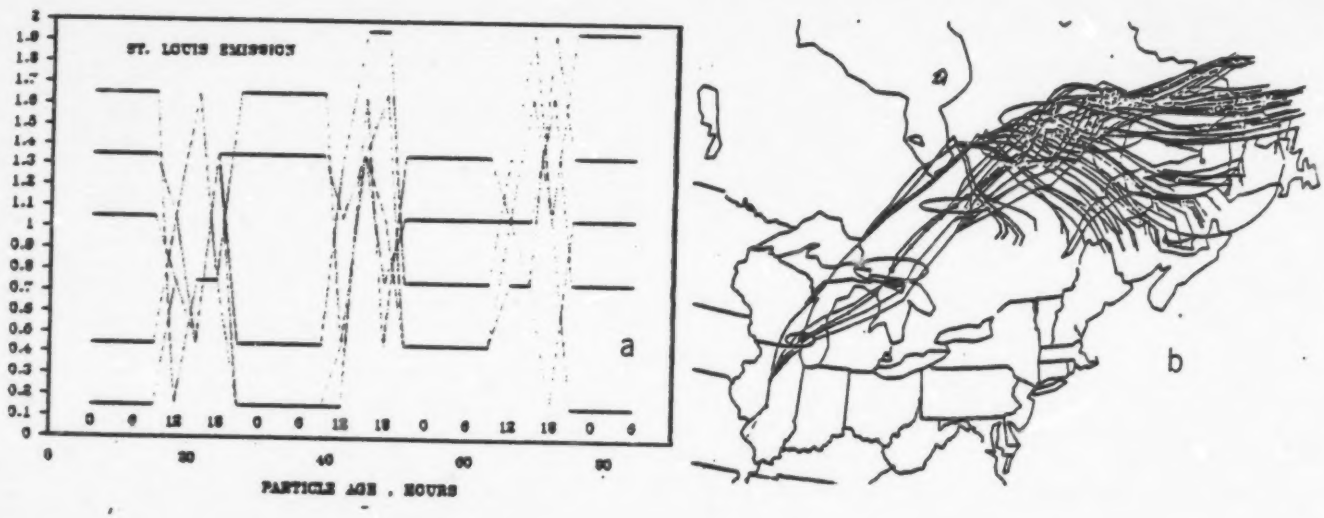

Figure 14. a) Time-height history for five particles. b) Trajectories of a 100 particle puff subjected to wind veer, shear, and vertical mixing.

surface) and high-level (tall stack) emissions.

Kinetics. The kinetic rate constants for SO_2 oxidation and SO_2 and SO_4 dry and wet deposition are obtained by fitting the model to pertinent current data sets. These include SO_2 and SO_4 concentration data from the Sulfate Regional Experiment (SURE) and the Regional Air Pollution Study (RAPS), as well as wet deposition data from five current precipitation chemistry networks. All rates vary seasonally. The dependence of the 3-hourly rate constants on the numerous parameters listed in Table 1 is illustrated for two particle histories in Figure 15a. In addition to the diurnal variation there is also a day to day variation of the conversion rate as influenced by the solar radiation (total sky cover). The resulting sulfur budget for the same puff emitted by a near-surface source in early night is shown in Figure 15b. The initial strong SO_2 decay is due to dry deposition depletion in the shallow nocturnal boundary layer. The conversion to sulfate only begins at the onset of the next day. The sharp decline of SO_4 at age 95h is due to the passage of the puff through a precipitation event. For the particular puff illustrated for a St. Louis summer release, about 25% of the SO_x has been converted and wet deposited as SO_4. The remainder 75% was mostly dry deposited as SO_2. In a companion graph (15c), the sulfur budget is illustrated for a puff from a tall stack source (300m effective stack height). For the initial 15 h, the puff rides over the nocturnal mixing layer, experiencing no dry deposition and only slow (0.5 %/h) SO_2 conversion rate. This initial delay increases the atmospheric lifetime (1/e) by 50% compared to the surface source. Hence, these graphs illustrate our approach to simulating the effect of tall stacks on the SO_x lifetime and transport distance. In general, it can be stated that the role of stack height is pronounced only for night time emissions.

The role of effective stack height is further illustrated in Figure 16a,b, by comparing the dry + wet deposition fields around the St. Louis source from a tall and low stack source. It is apparent that during the July dispersion and kinetic conditions, the deposition field gradient is much steeper for the surface source than from the tall stack source. For the January simulation, this difference in stack heights does not change the deposition field significantly. The role of stack height on the sulfur deposition with distance may be estimated by plotting the cumulative fraction of dry plus wet deposition versus increasing radial distance from the source, which approaches unity at infinite distance. The characteristic transport scale may be defined as the distance from the source at which 66% of the sulfur has been deposited. Such cumulative plots for July and January upper and lower sources and a St. Louis origin is given in Figure 17. The shortest transport distance of 700 km arises from a surface source in July. The night time low source emissions are significantly depleted during their exposure to the surfaces. The surface emission in January is transported to 900 km. Interestingly, the characteristic sulfur transport distance of about 1100 km for a tall stack is comparable for a winter and summer emission. Thus, for a St. Louis source, the characteristic (1/e) sulfur transport distance is about 1000 km . The deposition field around each source is roughly eliptic in shape with major axis along the prevailing winds; the characteristic transport distance is different for each region, dictated by the local transport and precipitation fields.

Application. For retrospective modeling of sulfur concentrations and depositions, it was assumed that the tranport and precipitation meteorology for 1978 and 1980 were representative for the past 100 years. The limitations of this assumption are unclear.

The attribution of total sulfur deposition, D(i,j) at receptor site j to the responsible sources S(i) can be calculated as follows:

$$D(i,j) = t(i,j) * S(i)$$

Thus, the deposition D(i,j) (g S/m^2,yr) is proportional to the source strength, S(i) (g

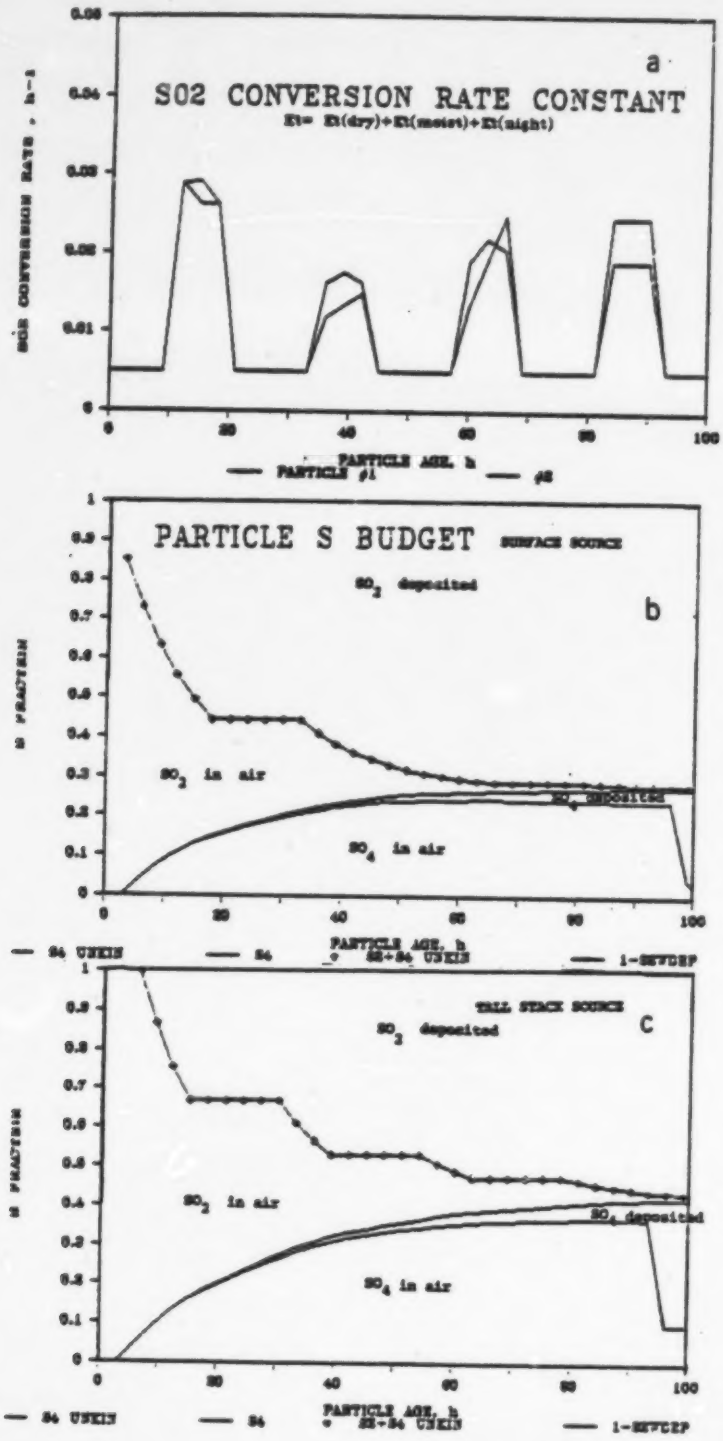

Figure 15. a) SO_2 conversion rate constant history for two selected particles. b) Sulfur budget for a low level source emitted at 1800 LST. c) Sulfur budget for tall stack source emitted at 1800 LST. For a tall stack emission, the dry deposition at night is zero.

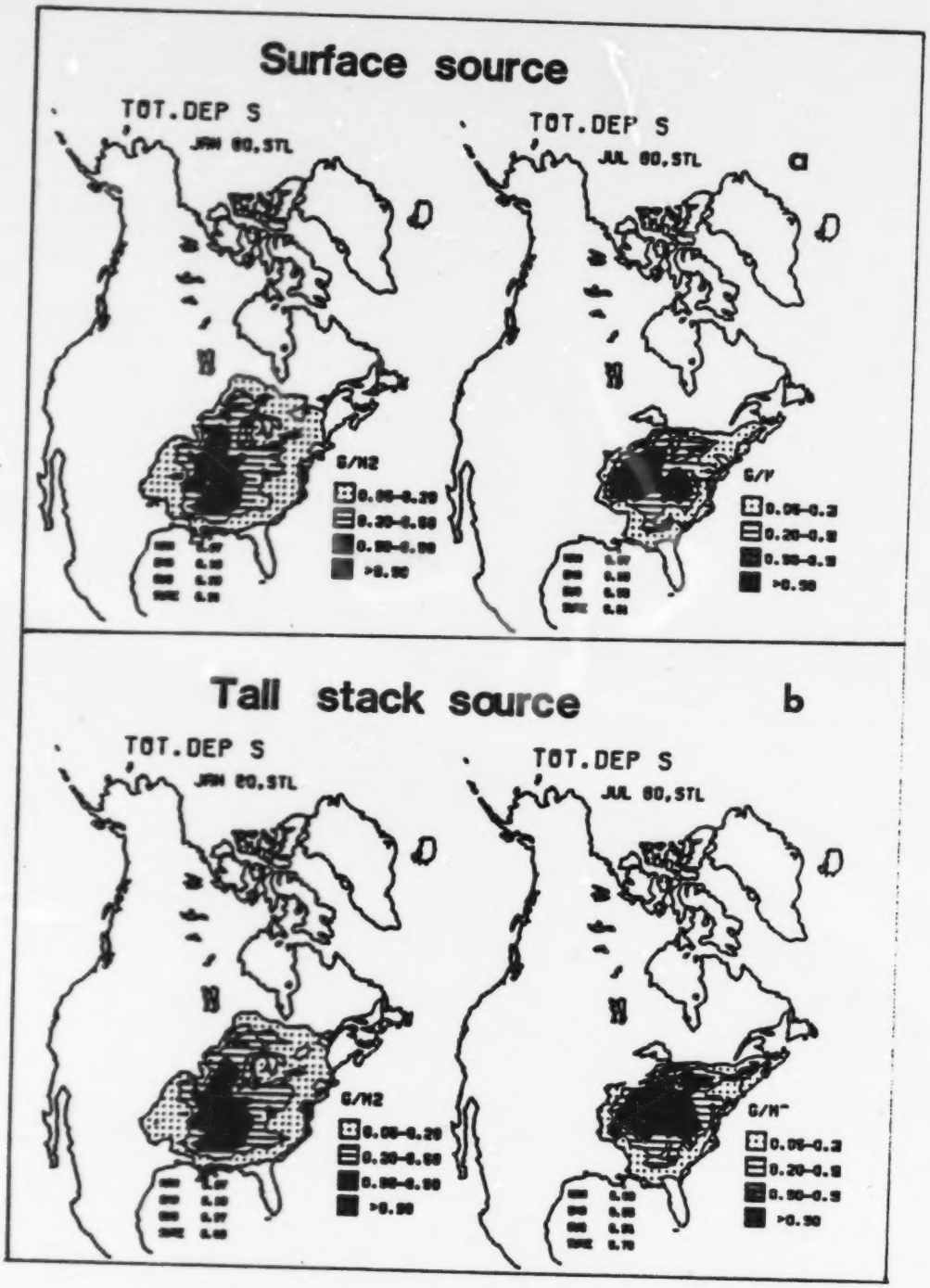

Figure 16. a) Deposition field for a surface source. b) Deposition for a tall stack source at St. Louis. For January, tall and short stack source have similar deposition pattern. For July, the tall stack emissions spread further.

S/m^2,yr), where the proportionality constant is the element of a transfer or source- receptor matrix, t(i,j). The physical interpretation of the transfer matrix is that it states the fraction of the matter emitted from a source at location (grid) i and deposited at receptor j. A transfer matrix element may also be envisioned as the probability that a molecule emitted at i will be deposited at j. The deposition at j from all i sources may be calculated as

$$D(j) = \sum D(i,j) = \sum t(i,j) * S(i)$$

The total deposition D(j) (g S $/m^2$,yr) is the sum of all the source strengths S(i) each weighed by its transfer matrix element t(i,j). This linearized formulation of source- receptor relationship assumes that deposition from one source occurs independently of other emissions. This assumption has been criticized in the past (Rodhe et al., 1981) on the grounds that the chemical compounds from one source influence the fate of emissions from other sources. However, both the participants of the 1982 Stockholm Conference on the Acidification of the Environment (1982) and the NAS report "Acid Deposition: Atmospheric Processes in Eastern North America, A Review of Current Scientific Understanding" concluded that the total deposition over an industrialized region (1000 km) will respond proportionally to emission changes.

The procedure of regional source attribution is illustrated graphically in the three maps of Figure 18. The emission density for SO_x shows highest values (> 8 g S/m^2,yr) over the Ohio River Valley. The center map shows the contours of constant transfer matrix elements for dry plus wet deposition for a receptor located in the Adirondack mountains. The third map is the product of the SO_2 emission density matrix times the transfer matrix. It will be called the source attribution matrix. It reveals the location of source areas that contribute most heavily to the sulfur deposition in the Adirondacks. The contours of the source attribution map have been drawn such that the blackened areas account for 25% of the deposition, while the lowest source attribution contour includes 90% of the Adirondacks deposition. According to these calculations, sources south of the Ohio and west of the Mississippi River contribute less than 10% of the Adirondacks deposition.

Similar procedures have been used to reconstruct the SO_2 concentrations and wet deposition rates for the New York City area for the past century.

For this application, the set of sources correspond to states rather than equally spaced grids, in order to match the scale of historical emission estimates. We thus implicitly assume that the relative source distribution within each state has not changed markedly. The two receptor grids which were used to represent "New York" are indicated as the rectangular areas of Figure 19. The receptor covers substantial portions of Connecticut and northern New Jersey; this is due to the 100 km resolution inherent in regional model simulation. The same figure also illustrates the SO_2 emission grid for area sources and point sources over the northeastern United States. It is seen that the area source emission density is very high in the New York City receptor grids, but that high density areas for point source emission include large portions of more remote states, e.g. PA and OH. Local grid emissions are dominated by area sources, which typically have lower effective stack heights than do point sources.

Figure 20 depicts the SO_2 concentrations for two extreme stack height scenarios: one scenario assumes that all sources emit the SO_2 near the surface, while the other assumes that all emissions are injected into 150- 450 m layers of the atmosphere. The latter, "tall stack" scenario constitutes an estimate of the lowest average SO_2 concentration that could exist for the given emission field. Indeed, those SO_2 concentrations would be low: 5-15 ug/m^3 S (or 10-30 ug/m^3 SO_2). The "low stack" scenario shows the concentrations to be about twice those of the tall stack case. However, it is emphasized here that the low stack case represents the highest average concentrations possible for the assumptions of the regional simulation. Specifically, in

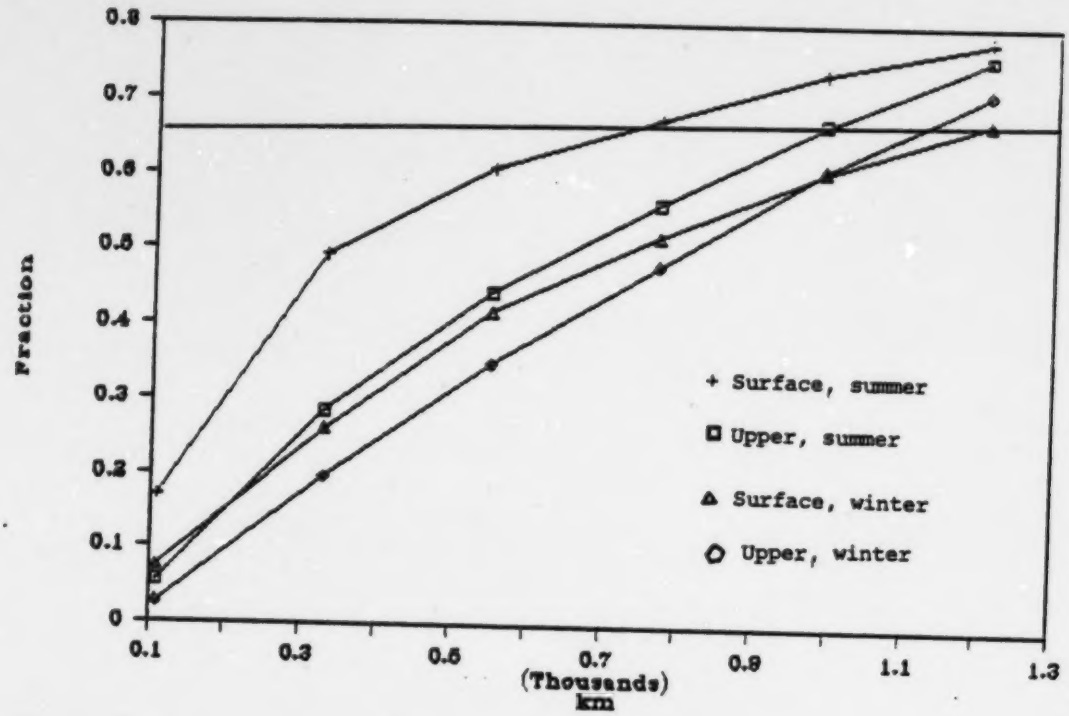

Figure 17. Cumulative dry + wet deposition from tall and short stack source. Only for summer emissions from a short stack is the transport distance significantly reduced.

the model the individual stacks are instantly dispersed over a 100 x 100 km grid, and are detected only at 3h intervals after instantaneous vertical mixing within the surface layer. The distribution of the regional simulation value may lead to much larger concentrations in small areas. Hence, the regional model tends to underestimate the surface SO_2 concentrations from nearby surface sources within a grid.

6. RECONCILIATION OF DATA AND MODEL ESTIMATES

In this section an attempt is made to reconcile the existing trends from observations with model estimates of SO_2 concentration. Figure 21 shows the SO_2 trends for NYC estimated by different methods. The lowest two lines (Xs and triangles) represent the regional model estimate for tall and short stacks respectively. These are identical to the values given in Figure 20. The top line (inverted triangles) shows the estimated maximum SO_2 concentration averaged over the New York City area (200 x 100 km). This maximum concentration was estimated from the local model to be three times higher than the surface concentration given by the regional model. According to such a scenario, the average surface concentration in the New York area would have ranged between 50 and 100 $\mu g/m^3$ S as SO_2 for the past 60 years. This scenario corresponds, for example, to sulfur sources that are distributed over a large area and emitted from small sources such as residential homes and railroads.

Figure 21 also contains area wide SO_2 data estimated from Eisenbud et al. It is evident that from 1958 to the early 1970s the SO_2 concentration was higher than that predicted from the regional model and lower than the upper estimate applicable to small area sources. In order

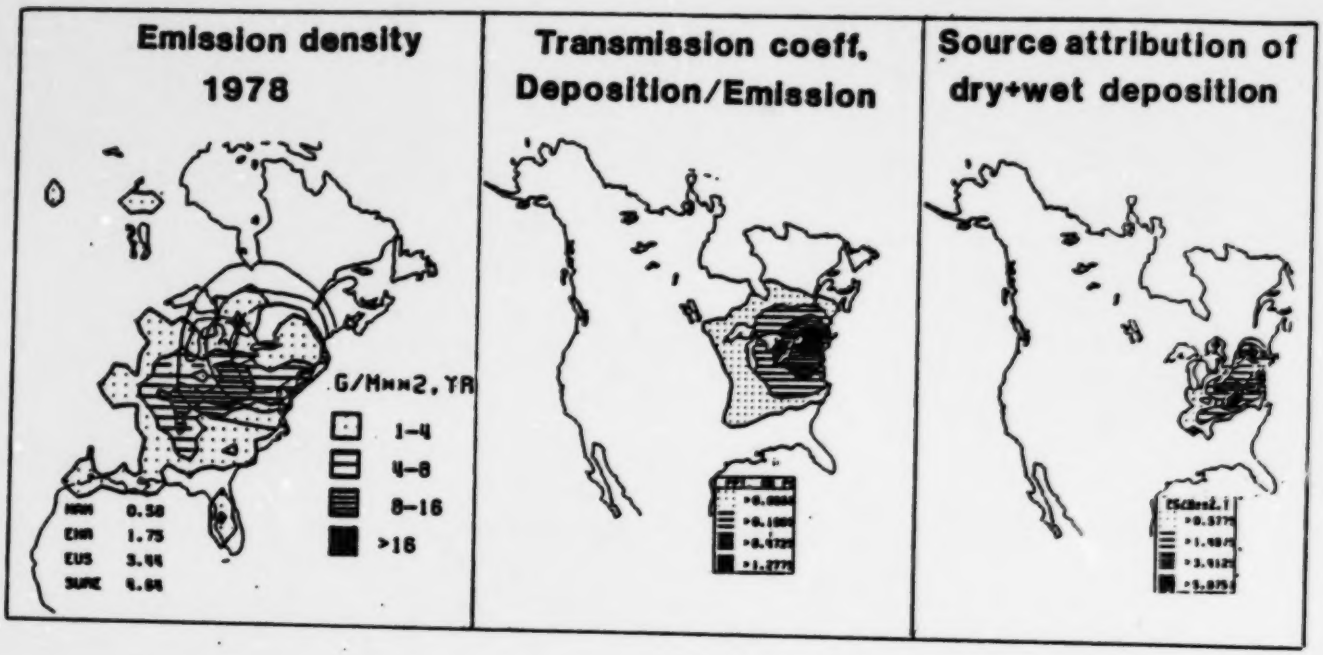

Figure 18. Source attribution of dry + wet deposition at the Adirondacks. a) Emission density for 1978. b) Unit transfer matrix. c) Source attribution map.

to incorporate this observation into the retrospective model, a "short stack" factor has been incorporated. Its value is such that the SO_2 concentration at any given time is the product of the regional model concentration times the short stack factor. The value of this factor was taken to be 3 in 1880, reflecting our assumption that in the 1900s all sources of SO_2 originated from short stacks with little thermal buoyancy per source. The factor was decreased linearly from 3 in 1880 to reach 2 in 1960. This decrease is based on the increase of the size of sources that emit the sulfur dioxide, causing increasing effective stack height due to buoyancy. The factor was then sharply reduced from 2 to 1.2 between 1960 and 1980. This reduction is assumed on the grounds of increasing physical stack height and thermal capacity buoyancy of major sources.

The "best estimate" SO_2 concentration for the New York City area, calculated by the above procedure, is also shown in Figure 21. Since the stack factor is between 1.2 and 3,the best estimate SO_2 concentration is higher than the regional model estimate but lower than the maximum. A noteworthy feature of these estimates is that the concentration in the 1970s is close to the concentrations given by the regional model. This again gives evidence for the regionalization of the SO_2 pattern.

The regional model was also used to estimate the wet deposition trend for the New York City area (Figure 22). Evidently, the wet deposition rate has been slowly increasing from about 0.6 g/m^2,yr in the 1920s to about 1 g/m^2,yr in the 1970s. As a reminder, these deposition rates are averages over a 200 x 100 km area. Small areas in the vicinity of sources can have much higher depositions.

Comparison of the wet deposition and SO_2 concentration trends in the New York City area shows a similar pattern until the mid 1960s (Figure 22). At that time the wet deposition was evidently rising and leveled off in the 1970s, while the SO_2 concentration has sharply declined

Reproduced from
best available copy.

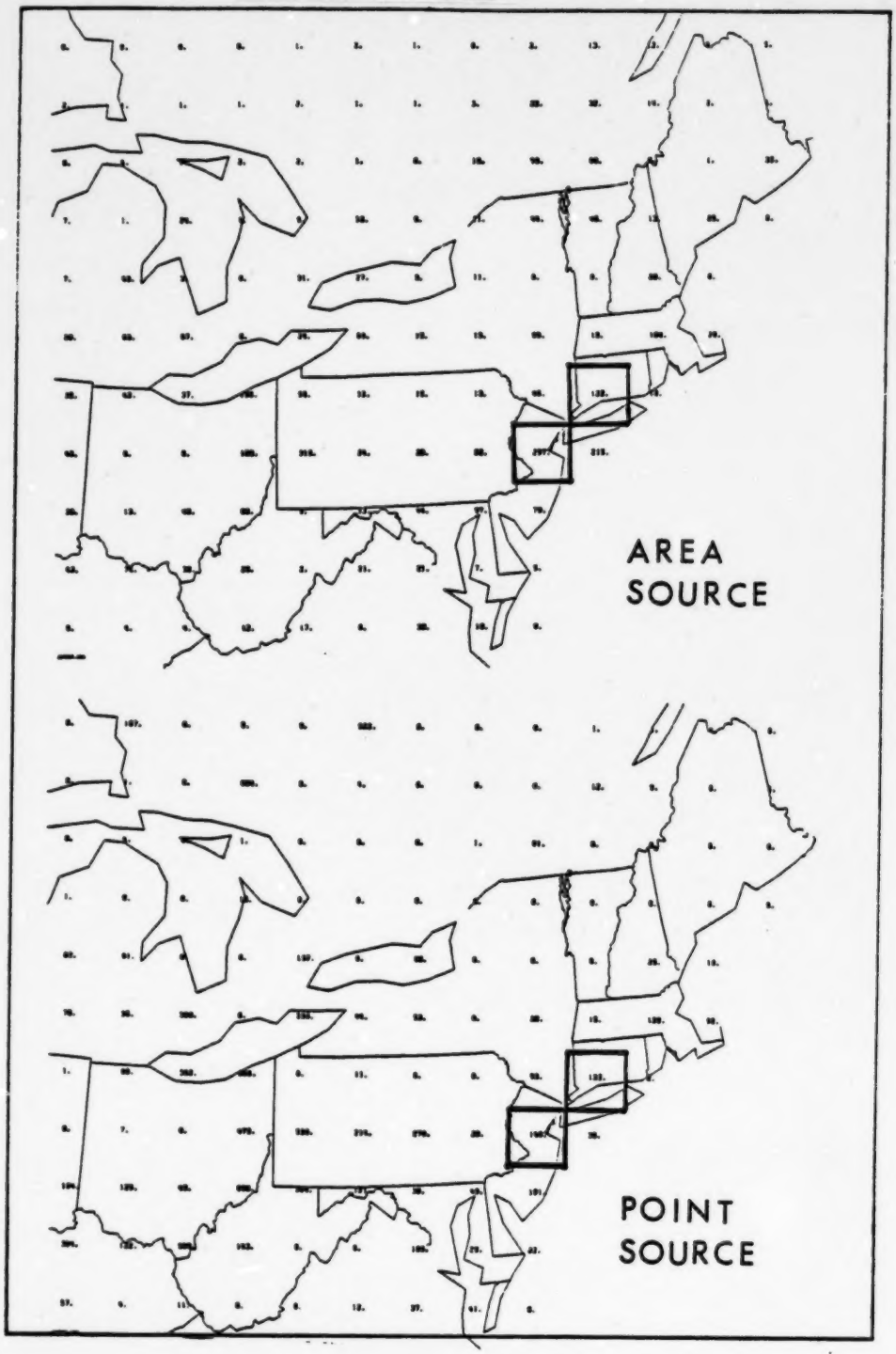

Figure 19. Regional model grids used for New York City area SO_x estimates. Numbers indicate SO_x emission densities for area sources (top) and for point sources (bottom).

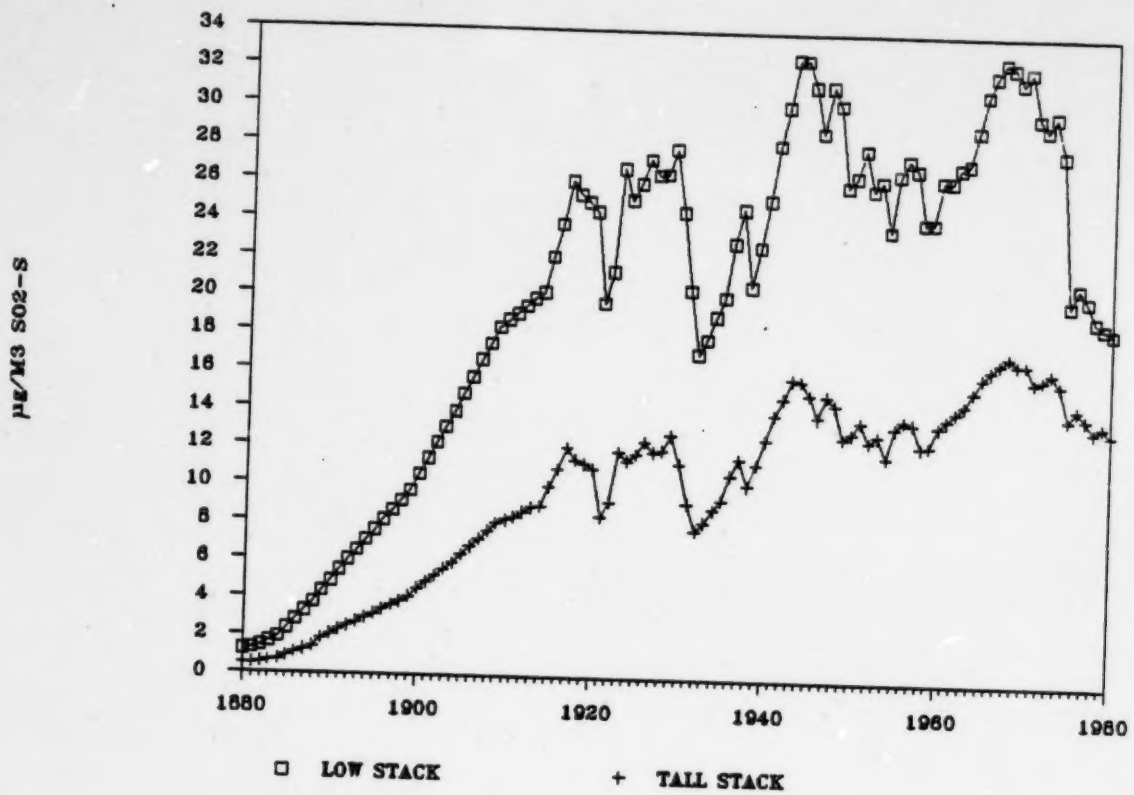

Figure 20. Regional model estimates of SO_2 concentration trend in the New York City area.

due to the "tall stack effect".

The above analysis of retrospective concentration estimates demands further discussion of uncertainties. The uncertainty of emissions is estimated to be about a factor of two around the turn of the century, declining for recent years. The spatial pattern of emissions in the New York City area has undoubtedly been changing since the turn of the century. It is probable that the emission field in the early decades of this century was much more concentrated around Manhattan. Consequently, it is also probable that the concentration ratios of Central Park to Cypress Hills and Long Island were actually higher in the early years. Prior to 1950, railroads contributed a significant fraction of the S emissions in the metropolitan area, but their contributions declined significantly by the 1950s. Unfortunately, we are not in position to quantify the effects of the above factors on the concentration trends at the two sites.

However, our interest here is focused on the early data sets (in the 1950s), because they may be representative of the general conditions before World War II. Specifically, we have used the Central Park measurements for 1958-1968 to establish a ratio between estimated emissions and resulting ambient concentrations at that site. We assume that this ratio was constant from 1890 to 1960.

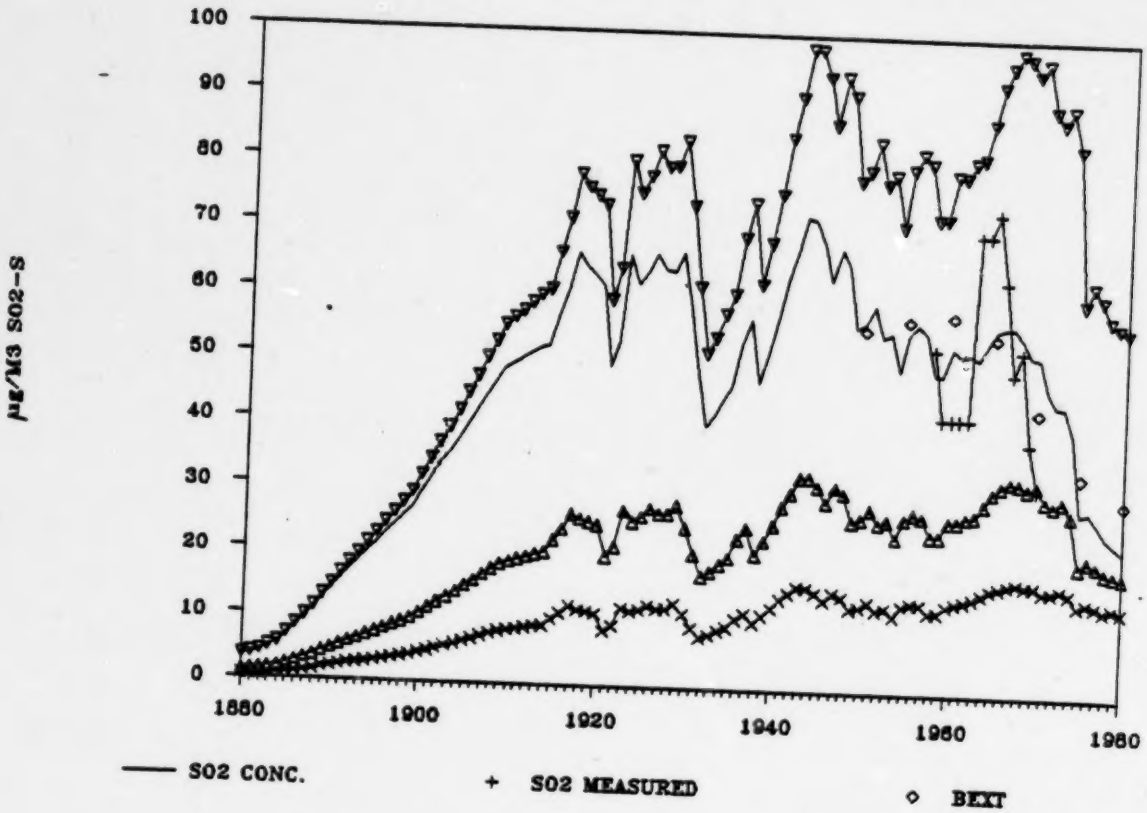

Figure 21. Reconciliation of measured SO_2 and b_{ext} with regional model SO_2 concentration. Regional model estimates: top line (triangles) is maximum SO_2 concentration from regional model; line with no symbols is best estimate of SO_2 concentration from model; lower curve with triangles is concentration from low level sources in regional model; bottom curve is regional model SO_2 concentration from elevated sources. Data: measured SO_2 concentration is line with crosses (X)and diamond symbols indicate trend of b_{ext}.

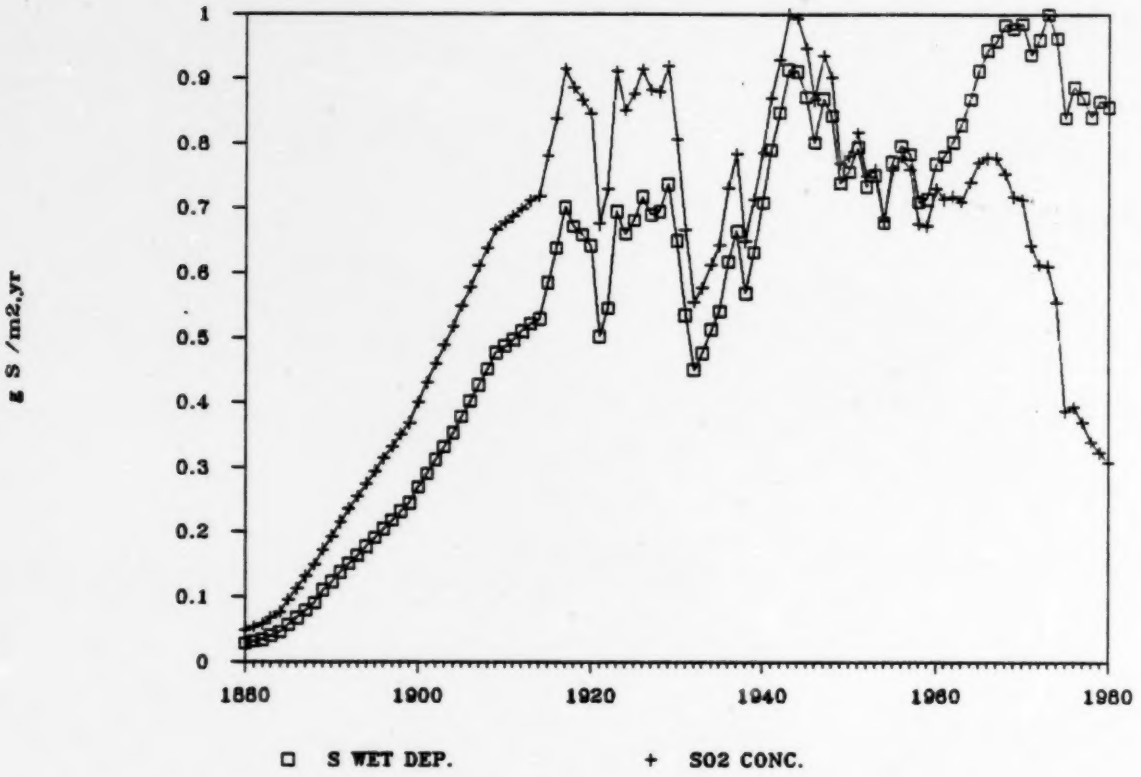

Figure 22. Comparison of regional model estimates for New York City area SO_2 concentration and S wet deposition.

7. DISCUSSION

It needs no elaboration that the estimation of local and regional emissions pertinent to a given receptor, the quantification of the local and regional contributions to SO_2 and to the wet deposition, and reconciliation of the above with the existing observations is a formidable task for current conditions. We are not aware of research results where the local and regional contributions were estimated for <u>current</u> conditions, and certainly not for historical trends. This, however, does not diminish the need for such estimates. Lacking data for the historical trends, many of the assumptions here are based on intuition or "best available science", and they should be revised with the availability of new knowledge.

REFERENCES

Rodhe, H. et al. (1981) Formation of sulfuric and nitric acid in the atmosphere during long range transport. Tellus, 33:132-141.

Patterson, D.E. et al. (1981) Monte Carlo simulation of daily regional sulfur distribution: comparison with SURE sulfate data and visual range observations during August,1977. J. Appl. Meteor. 20:404-420.

Holzworth, G.C. (1972). Mixing heights, wind speeds, and potential for urban air pollution throughout the contiguous United States. US EPA AP-101.

Portelli,R.V. (1977). Mixing heights, wind speeds and ventilation coefficients for Canada. Environment Canada, AES Climatological Studies # 31, UDC:551.554.

MOI (1982). Emissions, Costs, and Engineering Assessment: Work group 3B, U.S.- Canadian Memorandum of Intent.

Acidification Today and Tomorrow (1982). Proceedings of the 1982 Stockholm Conference on the Acidification of the Environment, p 103.

NAS (1983). Acid Deposition: Atmospheric Processes in Eastern North America. National Academy of Sciences, Washington, DC.

NAS (1985). Monitoring and Assessment of Trends in Acidic Deposition. To be published. National Academy of Sciences, Washington, DC.